

# We are IntechOpen, the world's leading publisher of Open Access books Built by scientists, for scientists

6,900

Open access books available

185,000

International authors and editors

200M

Downloads

Our authors are among the

154

Countries delivered to

TOP 1%

most cited scientists

12.2%

Contributors from top 500 universities



WEB OF SCIENCE™

Selection of our books indexed in the Book Citation Index  
in Web of Science™ Core Collection (BKCI)

Interested in publishing with us?  
Contact [book.department@intechopen.com](mailto:book.department@intechopen.com)

Numbers displayed above are based on latest data collected.  
For more information visit [www.intechopen.com](http://www.intechopen.com)



# The Use of Matlab in the Study of the Glass Transition and Vitrification in Polymers

John M Hutchinson and Iria Fraga  
*Universitat Politècnica de Catalunya  
Spain*

## 1. Introduction

The glassy state of matter is common to all types of materials, be they metallic, inorganic or polymeric, for example. The transformation from an equilibrium liquid state to a non-equilibrium glassy state is usually achieved by cooling at a rate sufficiently rapid for crystallization to be inhibited. For metals, this generally requires cooling rates of the order of millions of degrees per second, whereas, for polymers that can crystallize, a glassy state can be achieved with cooling rates of only hundreds of degrees per second. Furthermore, for atactic polymers the irregularity of the chemical structure prevents crystallization and results naturally in an amorphous glassy state. Cooling is not the only way in which a glassy state can be achieved, though. The application of high pressure is another method, though it is rather rarely used for reasons of experimental difficulty and danger. On the other hand, an alternative method that is very commonly used is by means of a chemical reaction, and in particular the curing reaction of a thermosetting polymer. In the present paper we concentrate on the glass transformation process by these two commonly applied methods, namely cooling from the equilibrium liquid-like state and vitrification during the cross-linking reaction of a thermosetting polymer.

The glassy state is characterized by a lack of long range order, and is also referred to as an amorphous state. This does not, however, mean that there is no discernible structure of the glass; on the contrary, there is a structure to the glass, which can be quantified in respect of its short range order, and this structure is dependent on the way in which the glass was formed. A good example of this is the preparation of densified glasses by cooling from the melt state to the glassy state under high pressure and then releasing the pressure; the density, and other properties, of the glass formed under pressure in this way is greater than, and remains greater than, that of the glass formed from the same melt by cooling at atmospheric pressure. The fact that the structure of the glassy state depends on the way in which the glass was formed is important, because the properties of the glass are, in their turn, dependent on the structure.

A further important characteristic of the glassy state is that it is a non-equilibrium state. This was first recognized by Simon (Simon, 1931) the best part of a century ago, who proposed that, on cooling the equilibrium liquid at constant pressure, a transformation to a glass takes place at a temperature, known as the glass transition temperature,  $T_g$ , when the timescale for molecular rearrangements, which increases as the temperature decreases, becomes longer than that available corresponding to the imposed cooling rate. An immediate consequence

of this is that the glass transition is a kinetic phenomenon, and that  $T_g$  depends on the cooling rate. Another consequence is that, if the temperature is held constant in the glassy state, the non-equilibrium glass will tend towards an equilibrium state at the same temperature. Thus, for example, the volume and the enthalpy of the glass will decrease as a function of time, in a process known as physical aging (Hutchinson, 1995), with consequent effects on other physical and mechanical properties. It is clearly of interest, therefore, not only from a fundamental scientific point of view but also with respect to the engineering applications of polymers, to be able to describe quantitatively the kinetic nature of the glass transition and the time dependence of the property changes that take place during physical aging.

The basic equations describing these kinetic aspects derive from the early experimental studies conducted by Tool in the 1930's and 1940's on silicate glasses (Tool, 1946, 1948; Tool & Eichlin, 1931), and later by Kovacs on polymer glasses (Kovacs, 1963), both making use of dilatometry. From these studies, two key features of structural relaxation of glasses were identified. First, Tool established that the relaxation time for structural relaxation of glass was dependent not only on the temperature but also on the instantaneous structure of the glass, and he proposed that the structure be characterized by the fictive temperature,  $T_f$ , to be defined below. Second, Kovacs showed that the relaxation process involved a distribution of relaxation times. Although nowadays such experiments are almost invariably made by Differential Scanning Calorimetry (DSC), the phenomenology is the same, and these two key features are necessary for any realistic description of the kinetics of structural relaxation. For reasons that will become clear later, they are now commonly referred to as non-linearity and non-exponentiality, respectively. In this paper, we apply a relatively simple theory for structural relaxation, in which these two aspects are intrinsic, to explore a number of different situations of practical importance involving the kinetic response of polymers in the glassy state, including the effect of cooling rate on the glass transformation process for polymers of different types, the relationship between cooling rate and frequency derived from Temperature Modulated DSC (TMDSC), and the identification of vitrification during the cure of thermosetting polymers. For all of these simulations we make use of Matlab and demonstrate the usefulness and ease of application of several of its basic attributes.

## 2. Theoretical aspects

The basic kinetic equation assumes that the rate of approach to equilibrium is proportional to the departure from equilibrium. For DSC, the departure from equilibrium is the difference between the instantaneous enthalpy,  $H$ , which is a function of both temperature  $T$  and time  $t$ , and the value of the enthalpy in equilibrium at the same temperature,  $H_\infty$ , and is denoted as  $\delta = H - H_\infty$ , and hence:

$$\frac{d\delta}{dt} = -\frac{\delta}{\tau(T, T_f)} \quad (1)$$

In this equation  $\tau$  is the relaxation time, which depends on both temperature and fictive temperature according to the original suggestion of Tool. The fictive temperature is defined as that temperature at which the glass would have an equilibrium value of enthalpy if it were immediately removed to that temperature. This is illustrated in the simulated cooling curve shown as an enthalpy-temperature diagram in Figure 1.

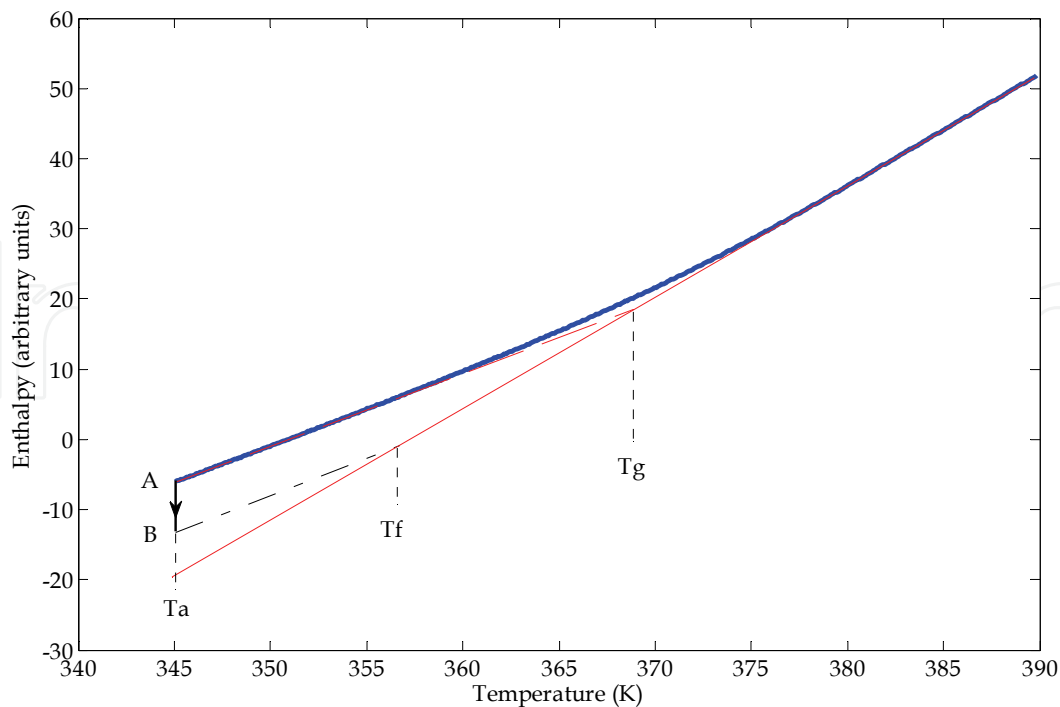


Fig. 1. Simulation of a DSC cooling curve, enthalpy versus temperature, showing the definitions of  $T_g$  and  $T_f$ . Parameter values: cooling rate  $-10$  K/min,  $\beta=0.4$ ,  $x=0.4$ ,  $\Delta h^*/R=85$  kK,  $\tau=100$  s at  $T_f=370$  K. The full red line is the asymptote to the equilibrium liquid region; the dashed red line is the asymptote to the glassy region

In this simulation, the glass is formed by cooling at  $-10$  K/min from 390 K to 345 K (state A), and from this cooling curve the glass transition temperature,  $T_g$ , is defined as the intersection of the equilibrium liquid and glassy asymptotes, as shown. If the cooling is arrested at A and the glass allowed to approach equilibrium isothermally by physical aging at the temperature  $T_a$ , a state B will be reached after some time. The state of the glass at B is defined conveniently by the fictive temperature,  $T_f$ , which is found as the intersection with the equilibrium asymptote of a line (dash-dotted) with the slope of the glassy asymptote and passing through state B. Various important aspects of the fictive temperature can be identified from this diagram: first, the fictive temperature of the glass in state A, immediately after cooling and forming the glass and without any physical aging, is identical to the glass transition temperature; second, as the glass is aged at the temperature  $T_a$ , below  $T_g$ , the fictive temperature decreases and in the limit is equal to the aging temperature; and third,  $T_f$  is related to  $\delta$  by:

$$\delta = \Delta C_p (T_f - T_a) \quad (2)$$

where  $\Delta C_p$  is the heat capacity difference between that of the liquid,  $C_{pl}$ , and that of the glass,  $C_{pg}$ .

Equation 1 introduces in a general way the dependence of the relaxation time on both the temperature and the fictive temperature of the glass, and is known as the single relaxation time model (Hutchinson & Kovacs, 1976). The specific dependence of  $\tau$  on  $T$  and  $T_f$  is usually written in one of two ways. In the TNM equation (Moynihan et al, 1976; Narayanaswamy, 1971; Tool, 1946), the dependence is written in the form:

$$\tau(T, T_f) = \tau_g \exp \left[ \frac{x\Delta h^*}{RT} + \frac{(1-x)\Delta h^*}{RT_f} - \frac{\Delta h^*}{RT_g} \right] \quad (3)$$

where  $\tau_g$  is the average relaxation time in equilibrium at  $T_g$ ,  $x$  ( $0 \leq x \leq 1$ ) is the non-linearity parameter,  $\Delta h^*$  is the apparent activation energy at  $T_g$ , and  $R$  is the universal gas constant. An alternative expression derives from the concept of configurational entropy (Gibbs & DiMarzio, 1958) and is known as the Adam-Gibbs (AG) equation (Adam & Gibbs, 1965):

$$\tau = A \exp \left[ \frac{N_A s_c^* \Delta \mu}{k T S_c} \right] \quad (4)$$

where  $N_A$  is Avogadro's number,  $s_c^*$  is the configurational entropy of the smallest cooperatively rearranging region that permits the transition of a molecular segment from one state to another,  $\Delta \mu$  is the elementary activation energy per segment,  $k$  is Boltzmann's constant and  $S_c$  is the macroscopic configurational entropy of the sample.

To introduce a distribution of relaxation times, two approaches are possible: by means of a discrete distribution, as in the so-called KAHR model (Kovacs et al, 1979), or, much more commonly and mathematically more conveniently, by means of an empirical distribution function, namely the stretched exponential or Kohlrausch-Williams-Watts (KWW) function (Kohlrausch, 1866; Williams & Watts, 1970):

$$\varphi(t) = \exp \left[ - \left( \frac{t}{\tau} \right)^\beta \right] \quad (5)$$

where the exponent  $\beta$  is inversely related to the width of the distribution of relaxation times. The set of equations 1, 2, 3 and 5 (or 1, 2, 4 and 5) is sufficient to simulate the response of a glass forming system to any prescribed thermal history. Matlab provides a very convenient environment in which to do this, and the results of such simulations in a variety of practical situations form the basis of this paper. In the first instance, the simple "three step cycles" thermal history is analysed, involving cooling at constant rate through the glass transition region to form the glass, isothermal annealing for various times to age the glass, and then reheating at constant rate through the transition region to simulate a typical DSC experiment, and in particular to examine the effects of the length of aging time at  $T_a$  on this reheating stage. Following this basic analysis of conventional DSC, the same procedure will be used to investigate the technique of TMDSC, in which a (usually) sinusoidally periodic modulation of the temperature is superimposed on the underlying cooling or heating rate (or isotherm).

### 3. Three step cycles

In this section, we outline first how the theoretical model can describe all the phenomenological aspects of the glass transition, and then show how the material parameters may be derived from experimental data by appropriate methods.

#### 3.1 Phenomenology

A typical simulated cooling curve has been shown in Figure 1, together with an unspecified annealing period at temperature  $T_a$ . The three step thermal cycles consist of these two steps followed by heating at constant rate, which is the step that is obtained experimentally by

DSC in the study of the physical aging or enthalpy relaxation of polymer glasses (Hodge, 1994; Hutchinson, 1995). These cycles are therefore defined by several experimental variables: the cooling rate,  $q_1$ , the temperature  $T_a$ , the aging time,  $t_a$ , at  $T_a$  (or the enthalpy reduction during this time,  $\bar{\delta}$ ), and the heating rate,  $q_2$ . In addition, there are several material parameters, the most important of which are:  $x$ ,  $\beta$ ,  $\Delta h^*$ ,  $\tau_g$  and  $\Delta C_p$ . The heating step of these cycles is dependent on all of these variables, and the purpose of these simulations is, first, to describe and explain the experimentally observed behaviour, and subsequently to show how to obtain the material parameters from the experimental data. Figure 2 (full lines) shows two typical heating curves, for glasses aged for about one month (blue line) and four months (red line) at a temperature  $20^\circ\text{C}$  below  $T_g$ , in which large endothermic peaks appear. This is the most important characteristic of such experiments, and the magnitude and position of these peaks reflects the amount of aging that has taken place at  $T_a$ . To determine the amount of enthalpy lost during aging, it is necessary to do a second cycle, cooling at the same rate as for the first cycle, and then immediately reheating at the same rate as for the first cycle, without any aging time at  $T_a$ . This second heating stage is sometimes called the reference scan, and is shown in Figure 2 by the dashed line (green). Although hardly visible on the scale of this figure, there is in fact a small endothermic peak, referred to as an upper peak (Hutchinson & Ruddy, 1990) and here centred at about  $65^\circ\text{C}$ , even though there has been no aging; it can be shown that such a peak must always be present in these heating scans (Ramos et al., 1984) unless it is hidden under the main endothermic peak. The difference in areas under the first and reference scans is equal to the enthalpy lost during aging at  $T_a$ .

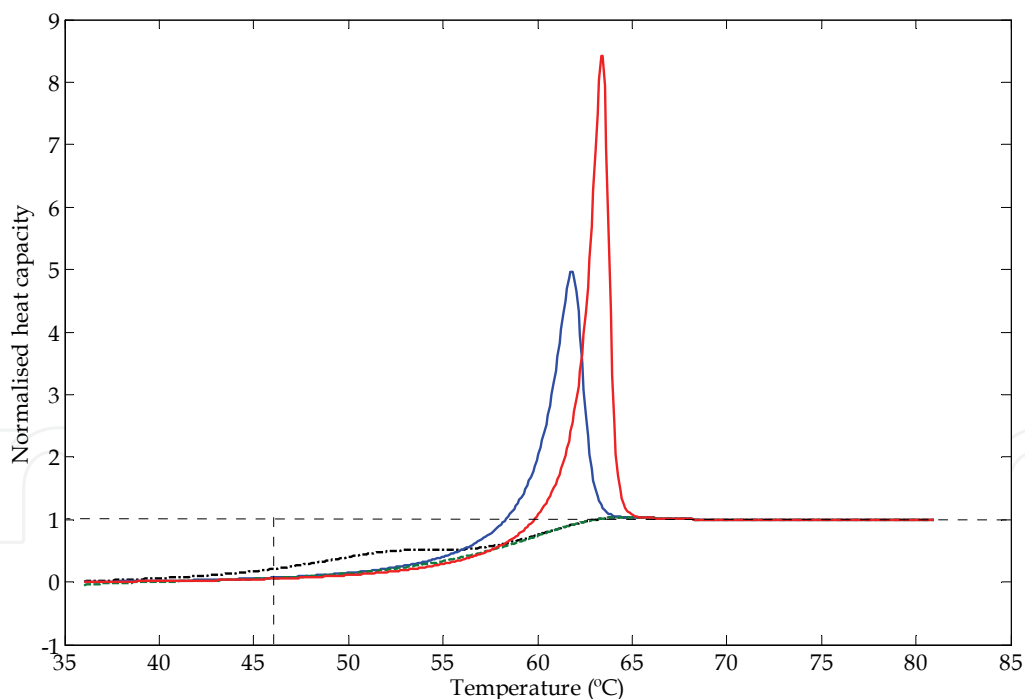


Fig. 2. Simulation of a DSC heating curve, normalised heat capacity versus temperature, for a glass formed by cooling at  $-40\text{ K/min}$  and then aged at  $T_a=36^\circ\text{C}$  for  $10^4\text{ s}$  (black dash-dotted line),  $3\times 10^6\text{ s}$  (blue full line) or  $10^7\text{ s}$  (red full line). Material parameter values:  $\beta=0.35$ ,  $x=0.4$ ,  $\Delta h^*/R=85\text{ kK}$ ,  $\tau=100\text{ s}$  at  $T_r=56^\circ\text{C}$ . The horizontal dotted black line is the asymptote to the equilibrium liquid region, and the vertical dotted black line indicates the fictive temperature,  $T_f$ , after aging at  $T_a$  for  $3\times 10^6\text{ s}$

The fictive temperature of the glass in the aged state, for example in Figure 2 after about one month at  $T_a$ , can be found by the so-called equal areas method (Moynihan et al., 1976; Richardson & Savill, 1975). In this method, illustrated in Figure 2, the total area under the endothermic peak for the aged glass is equal to the area under the asymptote to the liquid-like region (dotted black line) and above the fictive temperature,  $T_f$ . Clearly, with increased aging, as the endothermic peak increases in magnitude, the fictive temperature moves to lower values, and in the limit will asymptotically approach the aging temperature,  $T_a$ .

The same Figure 2 also shows another characteristic feature of the heating scan of glasses which occurs under certain conditions. The dash-dotted black line is the heating scan following only about 3 hours aging at  $T_a$ , and shows the existence of what is often called a sub- $T_g$  peak, here at about 52.5°C. When first observed by DSC, the appearance of double peaks in the glass transition region was considered something of a mystery (Illers, 1969; Neki & Geil, 1973; Retting, 1969), though they in fact arise quite naturally as a consequence of the distribution of relaxation times, and under certain quite well defined experimental conditions: a fast cooling rate in comparison with the subsequent heating rate, and little or no aging at the lower temperature of the cycle, the lower this temperature relative to the glass transition temperature the more likely being the appearance of a sub- $T_g$  peak. In addition, although sub- $T_g$  peaks are often observed for glasses with low values of  $\beta$ , in other words when the relaxation time distribution is broad (Ruddy & Hutchinson, 1988), such as is the case for poly(vinyl chloride) (Berens & Hodge, 1982), a broad distribution of relaxation times is not a pre-requisite for their appearance, as was demonstrated by the behaviour of some carefully prepared inorganic glasses (Pappin et al., 1994).

This phenomenology of the response of glasses to heating through the transition region, in which characteristic features such as the endothermic peak and its dependence on the aging time and heating rate are observed, the existence of the upper peak and its relative invariance with the experimental variables (Hutchinson & Ruddy, 1990), and the appearance of sub- $T_g$  peaks and the conditions under which they are most likely to be observed, can be well described by the theoretical development outlined above. Simulations can be made very simply in the Matlab environment, and in particular, the ease of obtaining maximum values of a vector is of particular benefit. In the next section, these same simulations are used to show how the important material parameters may be derived from the experimental data.

### 3.2 The peak shift method

The theoretical development above includes one parameter in particular, the non-linearity parameter  $x$ , which, although defining the relative importance of temperature and structure (fictive temperature) to the relaxation time, does not have any obvious physical significance. Nevertheless, the excellent description of all the phenomenological aspects outline above suggests that there should be some physical significance, and considerable effort has been made by numerous workers to investigate this. The basic idea has been to evaluate  $x$  for different glass-forming systems in order to relate its value to the nature of the glass-former, and the review by Hodge (Hodge, 1994) gives an excellent summary. Fundamental to this approach is the need to have a reliable method for the evaluation of this parameter  $x$ . The majority of workers make use of what is termed the curve-fitting method, whereby a least-squares minimisation routine is used to fit the set of theoretical equations to the experimental DSC heating curve. While mathematically convenient, this approach suffers from some drawbacks: for example, it assumes a certain specific form for the distribution function, namely the stretched exponential. More importantly, though, it is often applied to

fit heating curves for glasses aged only for short times, which consequently have little non-linearity; it is not appropriate to determine the non-linearity parameter by fitting curves which have no significant dependence on this parameter.

An alternative approach, which does not suffer from these drawbacks, was proposed some time ago. It is based upon the dependence of the endothermic peak temperature,  $T_p$ , on the experimental conditions defining the three step thermal cycles (Kovacs & Hutchinson, 1979; Ramos et al., 1984). This has become known as the peak shift method. From an extensive analysis of the response of glasses to such cycles, the dependence of  $T_p$  on each experimental variable ( $q_1, T_a, \delta, q_2$ ) while maintaining the others constant was found, in the limiting case of long aging times, to be linear. Thus one can define a set of shifts  $[\hat{s}(q_1), \hat{s}(T_a), \hat{s}(\delta), \hat{s}(q_2)]$ , the most useful in respect of the experimental determination of  $x$  being:

$$\hat{s}(\delta) = \Delta C_p \left( \frac{\partial T_p}{\partial \delta} \right)_{q_1, T_a, q_2} \quad (6)$$

The interesting aspect of this approach is that these shifts are all inter-dependent, and are all functions of  $x$ :

$$F(x) = \hat{s}(\delta) = -\hat{s}(q_1) = \hat{s}(q_2) - 1 \quad (7)$$

where the function  $F(x)$ , in limiting conditions, asymptotically approaches the simple hyperbolic function  $F(x) = x^{-1} - 1$ , shown in Figure 3 and known as the master curve. Even more interestingly, this limiting function is essentially independent of the choice of distribution function used, be it a discrete distribution as in the multi-parameter KAHR model or the stretched exponential KWW function.

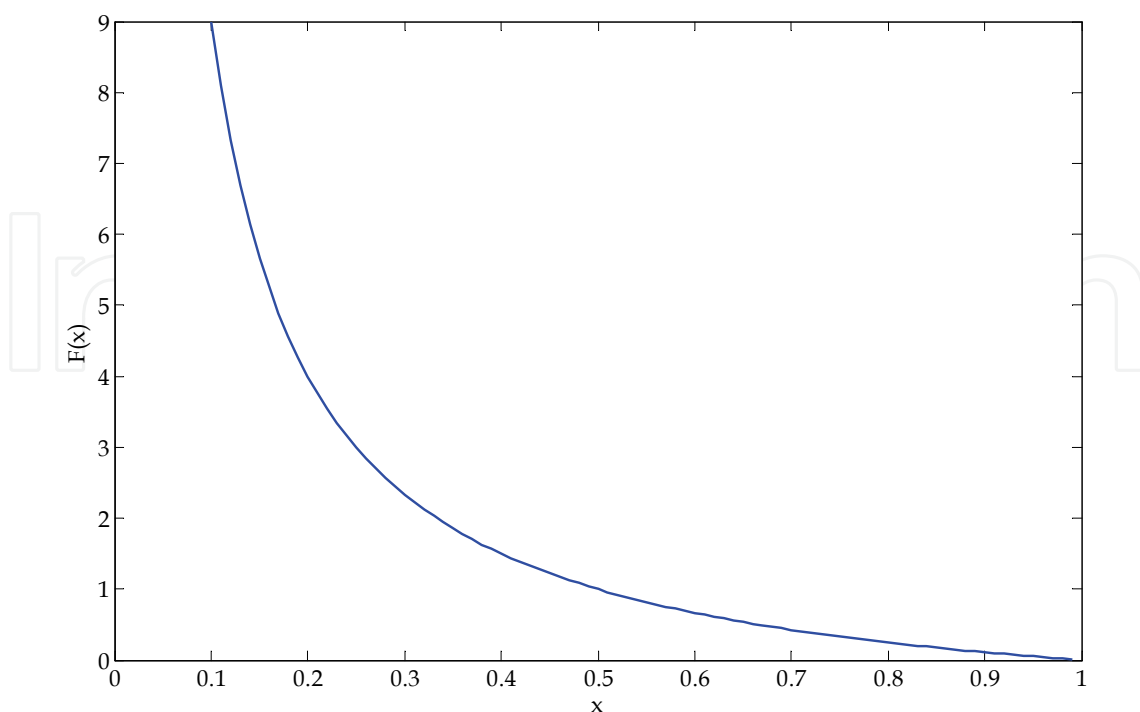


Fig. 3. Master curve for the peak shift method

The procedure (Hutchinson, 1987) is to determine, by a series of experiments, the peak endotherm temperatures,  $T_p$ , obtained on heating at constant rate, typically 10 K/min, for glasses which have been formed initially by cooling at the same rate, and then aged at a temperature,  $T_a$ , usually 10 to 20°C below  $T_g$ , for a range of times, which should extend ideally to periods as long as is convenient in order to approach the limiting conditions necessary. These lengths of time can be as much as several months, much longer than the timescales usually used in the curve-fitting method. For each endotherm, the associated enthalpy lost,  $\bar{\delta}$ , during the immediately previous aging can be determined from the area difference under this endothermic peak and under a reference scan made, for the same sample, under identical cycle conditions, but without any aging at  $T_a$ .

A plot of  $T_p$  as a function of  $\bar{\delta}$  or as a function of the logarithm of the aging time,  $t_a$ , appears linear for values of  $\bar{\delta}$  or  $t_a$  large enough for limiting conditions to be achieved, and from this linear region the slope is obtained which permits the evaluation of  $\hat{s}(\bar{\delta})$  from Equation 6, and hence of  $F(x)$  from Equation 7. The experimental value of  $x$  is then found from the master curve in Figure 3. The limiting dependence of  $T_p$  on  $\bar{\delta}$  is essentially independent of all the other experimental variables ( $q_1$ ,  $q_2$ ,  $T_a$ ) defining the thermal cycle, and of the distribution function for the relaxation times, and thus the peak shift method provides a rational means of evaluating experimentally the non-linearity parameter  $x$  (Hutchinson & Ruddy, 1988).

#### 4. Temperature modulated DSC (TMDSC)

In the early 1990s, the idea of modulating the constant heating rate of conventional DSC was conceived by Reading and co-workers (Gill et al., 1993; Reading et al., 1993a). It was patented in the US in 1993 (Reading et al., 1993b), and commercialised by TA Instruments as Modulated DSC. Subsequently, other instrument manufacturers commercialised their own versions, including Alternating DSC (ADSC) from Mettler Toledo. Generically, such techniques are now referred to as Temperature Modulated DSC (TMDSC). The basic principle in all cases is to superimpose on the constant heating rate (or cooling rate, or isotherm) of conventional DSC a periodically (and in practice sinusoidally) varying modulation. The idea is that, in addition to the same information as is available from conventional DSC, TMDSC also provides, at any time during a scan, information about the instantaneous state of the sample.

The periodically modulated heating rate and heat flow signals can be analysed by Fourier Transformation, to give the amplitudes of the periodically varying heat flow and heating rate signals, and an average heat flow signal. The average signal is essentially the same signal as would be obtained by conventional DSC at the same rate as the underlying rate of TMDSC; the ratio of the amplitudes of the heat flow and heating rate is sometimes referred to as the “reversing” component; and the difference between the underlying signal and the reversing component is known as the “non-reversing” component. An alternative approach is to treat the reversing component as a complex heat capacity,  $C_p^*$ , and use the phase angle which results from the Fourier Transformation to separate  $C_p^*$  into its in-phase,  $C_p'$ , and out-of-phase,  $C_p''$ , components (Schawe, 1995). With respect to the glass transition, the response of glasses in TMDSC during the heating stage of the three step thermal cycles shows some characteristic features: the average signal shows the usual endotherm associated with enthalpy relaxation which is seen by conventional DSC; the reversing component and  $C_p'$  show a sigmoidal change at an apparent glass transition temperature,  $T_g(\text{dynamic})$ , different

from that found by conventional DSC, and without any endothermic peak; the non-reversing component and  $C_p''$ , as well as the phase angle, show a peak in the region of  $T_g(\text{dynamic})$ . Although this technique of TMDSC appeared from the outset to offer several advantages over conventional DSC, the initial interpretation of some of these features of the response in the glass transition region was rather confusing. For example, the observation that  $T_g(\text{dynamic})$  is independent of the heating or cooling rate prompted the idea that this represented a rate independent  $T_g$ , in contradiction to the basic idea of the glass transition as a kinetic phenomenon, while the peak in the non-reversing heat flow was associated with enthalpy relaxation, since no peak appeared in the reversing component; this last, however, represents an interpretation difficult to reconcile with the fact that such a peak also appears in the non-reversing component during cooling, where enthalpy relaxation plays no part. There was clearly a need for a sound theoretical treatment of TMDSC in the glass transition region in order to interpret correctly the various signals. This could be based on the same formalism as had been adopted for the simulation of three step thermal cycles in conventional DSC, but now with a modulated temperature programme. These simulations were very conveniently made using Matlab, for which standard procedures exist for Fast Fourier Transformation (fft), for integrating the fundamental differential equation, Equation 1, for the kinetics of the relaxation process using the 4<sup>th</sup>-5<sup>th</sup> order Runge-Kutta routine (ode23), and for convolution integrals of the type required when the stretched exponential distribution is incorporated with the fictive temperature formulation (conv). Such simulations were able to describe quantitatively all the experimentally observed phenomena and thus permitted the interpretation of the signals in a logical way, as well as providing a means of investigating the effects of both the experimental and material parameters on the response. The most important aspects of these results are presented here.

The TMDSC experiment in the glass transition region is defined by a set of experimental parameters, which are: the underlying or average rate, either on cooling or heating ( $q_{av}$ ), the period of the modulations ( $p$ ), and the amplitude of the temperature modulations ( $A_T$ ). The material parameters are the same as those for the simulation of conventional DSC. As an illustration of these simulations, Figure 4 shows the result for a modulated cooling curve, in the form of modulated heat flow ( $HF$ ) as a function of time. It is clear that the amplitude of the modulations decreases markedly during cooling, corresponding to the sigmoidal change in the reversing or complex heat capacity. What is not so obvious is that the average value of the heat flow also decreases, though in a different way and over a different temperature (or time) range. In order to identify this effect, it is necessary to do a Fourier Transform (fft) of single cycles of these heat flow and heating rate modulations, using a window which is slid along the time scale to cover the whole cooling curve. From these Fourier Transformations, amplitudes and average values and the phase angle between heat flow and heating rate are obtained, from which the complex heat capacity and its in-phase and out-of-phase components, as well as the average heat capacity, are calculated:

$$C_p^* = \frac{A_{HF}}{A_\beta} \quad (8a)$$

$$C_p' = C_p^* \cos \varphi \quad (8b)$$

$$C_p'' = C_p^* \sin \varphi \quad (8c)$$

$$C_{P,ave} = \frac{\langle HF \rangle}{\langle \beta \rangle} \quad (8d)$$

In these equations,  $A_{HF}$  is the amplitude of the heat flow modulations,  $A_{\beta}$  is the amplitude of the heating rate modulations,  $\varphi$  is the phase angle between the heating rate and heat flow modulations, and  $\langle HF \rangle$  and  $\langle \beta \rangle$  are the average values of the heat flow and heating rate, respectively. Because the phase angle is very small in the glass transition region, the in-phase heat capacity is approximately equal to the magnitude of the complex heat capacity. The variations of the in-phase and out-of-phase heat capacities and of the phase angle, obtained by Fourier Transformation of the modulations in Figure 4, are shown in Figure 5.

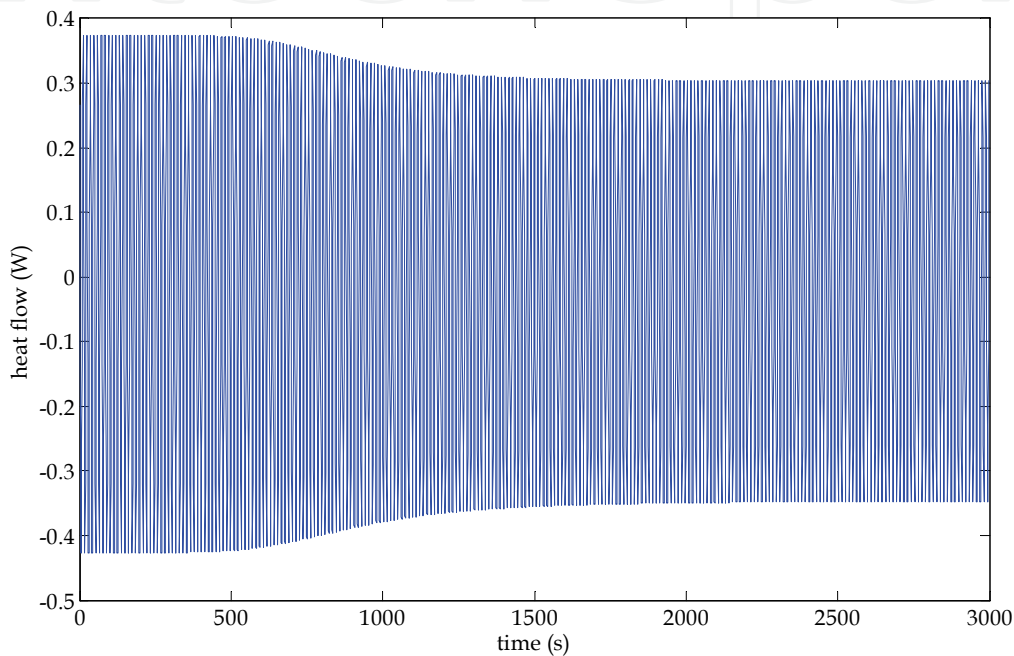
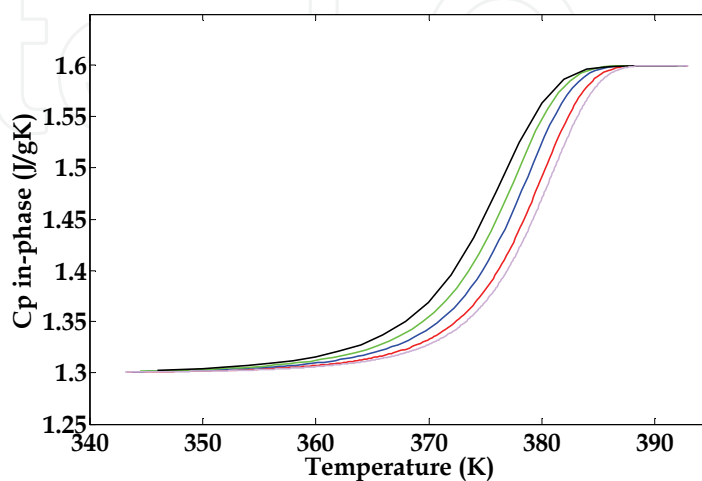
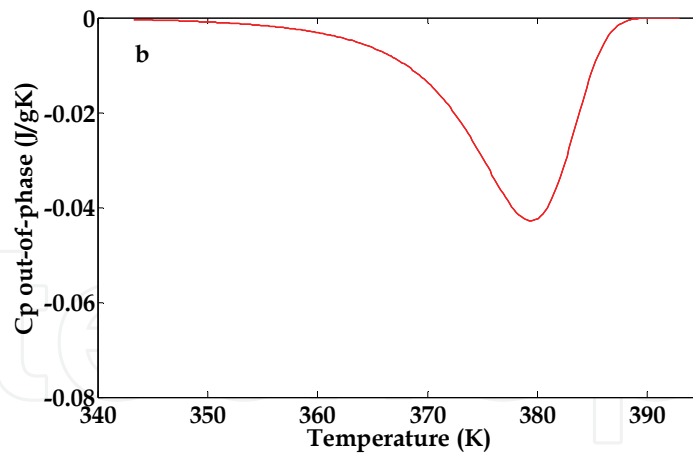


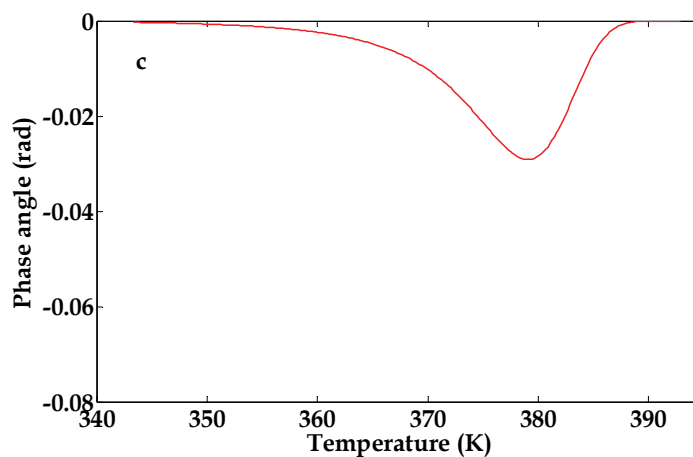
Fig. 4. Modulated cooling curve obtained by Matlab simulation with experimental and material parameters as follows:  $q_{av} = -1$  K/min,  $p = 12$  s,  $A_T = 0.5$  K,  $\beta = 0.4$ ,  $x = 0.4$ ,  $\Delta h^*/R = 85$  kK,  $\Delta c_P = 0.3$  J/gK,  $c_{PI} = 1.6$  J/gK,  $c_{Pg} = 1.3$  J/gK



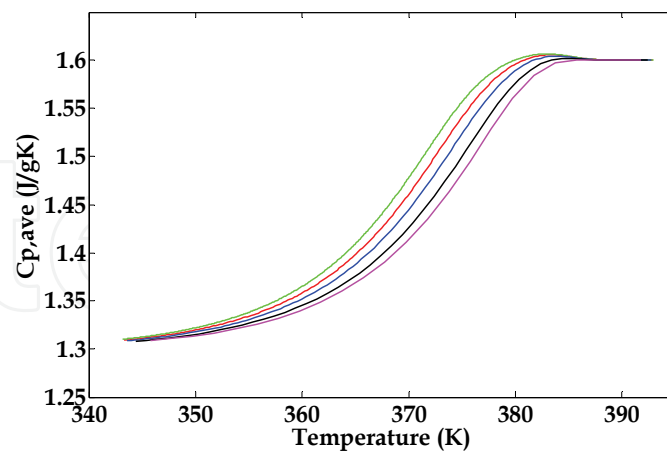
(a)



(b)



(c)



(d)

Fig. 5. Fourier transformed signals (red curves) for modulated cooling curve of Figure 4: (a) in-phase heat capacity; (b) out-of-phase heat capacity; (c) phase angle; (d) average heat capacity. In Figure 5a, modulation periods [s] are: 120 (black), 60 (green), 30 (blue), 12 (red), 6 (lilac). In Figure 5d, the cooling rates [K/min] are: -0.5 (green), -1 (red), -2 (blue), -5 (black), -10 (magenta)

The simulations of Figure 5 describe, both qualitatively and quantitatively, all the characteristic features of TMDSC experiments in the glass transition region. A number of comments may be made about these results in general, and also in respect of their dependence on both the experimental and material parameters. In the first place, it is evident that the dynamic glass transition (from  $c_p'$ , Figure 5a) is quite different from the conventional glass transition (from  $c_{p,ave}$ , Figure 5d). Not only is the former considerably sharper, but also the glass transition temperature, obtained for example from the mid-point (in these simulations, for the red curves where  $c_p = 1.45$  J/gK), is higher for the dynamic glass transition. These differences represent an important distinction between what are sometimes referred to as the thermal glass transition, from the average heat capacity of Figure 5d and equivalent to that obtained by conventional DSC, and the dynamic glass transition, from the complex or in-phase heat capacity of Figure 5a. In the former case, for the thermal glass transition, as the glass is cooled it departs from equilibrium (cf. Figure 1) at some temperature which depends on the cooling rate, and therefore the non-equilibrium state and the parameters describing non-equilibrium, in particular the non-linearity parameter  $x$ , play an important role in the kinetics of the transition. On the other hand, in the latter case, for the dynamic glass transition, the state is close to an equilibrium liquid in principle; the response of the sample is therefore glassy if the period of modulation is short, is liquid-like if the period is sufficiently long, and displays a transition region if the period is between these limits. The question of whether any given period is short or long has to be answered by comparing it with the instantaneous average relaxation time of the material. This average relaxation time increases as the temperature decreases, thus giving rise to the approximately Debye-type relaxation seen in Figure 5b for the out-of-phase component.

This situation is, however, complicated by the overlapping of the thermal and dynamic transitions, which can be demonstrated quite clearly by these Matlab simulations. It is a simple matter to run simulations for different values of period of modulation and of cooling rate to establish their separate effects, which are shown in Figures 5a and 5d, respectively. In Figure 5a, as the period of modulation increases, the dynamic glass transition temperature decreases, an effect which would, in principle, allow the determination of the apparent activation energy for the relaxation (Jiang et al, 1998). However, this determination of the activation energy supposes that the dynamic transition occurs entirely in equilibrium, analogous to the situation for dynamic mechanical analysis or dielectric analysis. However, it can be seen here from a comparison of Figures 5a and 5d that, even for the shortest modulation period of 6 seconds, the thermal transition begins before the dynamic transition has passed completely from a liquid to a glassy response.

There are two important conclusions that can be drawn from this observation. First, for the correct study of the dynamic glass transition, it is necessary to separate it from the thermal transition, which requires either a very slow cooling rate or a very short modulation period. The latter is limited by problems of heat transfer into the sample, and it is usually considered that the minimum period experimentally accessible is approximately 12 seconds. The former is limited only by available time, though it must be borne in mind that these experimental times can be very long; for example, the simulated experiment in Figure 5d for a cooling rate of  $-0.5$  K/min takes almost 2 hours, and it would require a further reduction in the cooling rate by at least an order of magnitude for the complete separation of the dynamic and thermal transitions.

These considerations lead to the second important conclusion, which is that there must be some equivalence between the cooling rate and the frequency of modulation, and that this

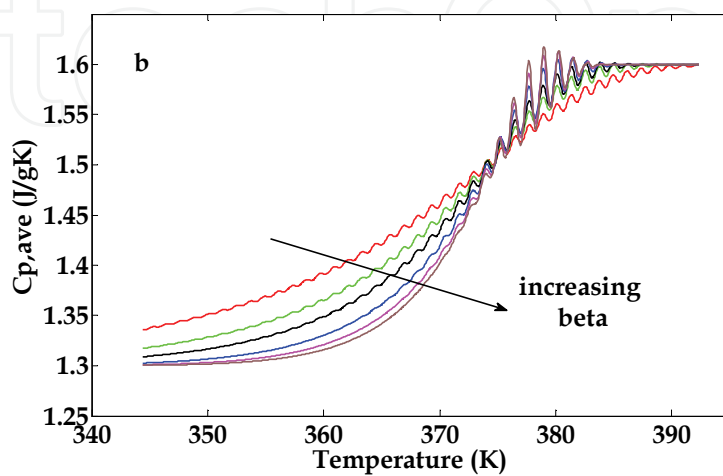
equivalence must be related to the material parameters,  $\beta$  and  $x$ . For example, it is almost always observed that, within what might be called typical ranges of values of the experimental variables (cooling rate and modulation frequency), these two types of transition overlap, with the dynamic glass transition usually being a few degrees higher than  $T_g$  (Donth et al, 1997; Hensel & Schick, 1998; Hutchinson, 1998; Montserrat, 2000; Weyer et al, 1997). A theoretical expression for the relationship between cooling rate and frequency can be derived from the fluctuation dissipation theorem for the glass transition (Donth et al, 1997), and can be written in the following form relating the angular frequency of modulation,  $\omega$  (rad/s) in TMDSC and the cooling rate  $|q|$  (K/s) in conventional DSC:

$$\omega = \frac{|q|}{a \delta T} \quad (9)$$

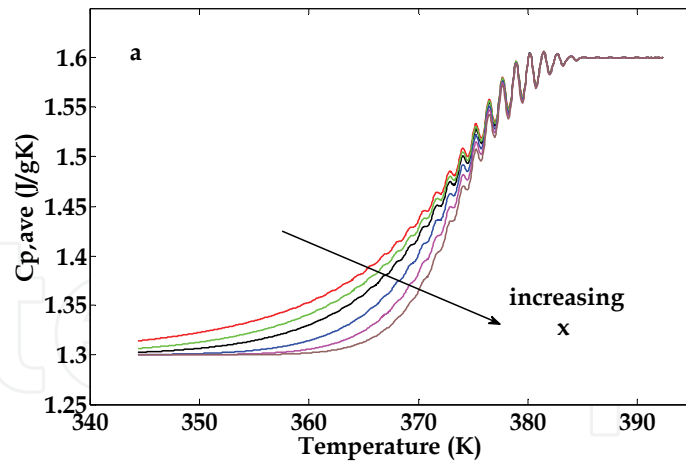
where  $a$  is a constant and  $\delta T$  is the mean temperature fluctuation of the cooperatively rearranging regions. By means of Matlab simulations in which the cooling rate in conventional DSC was determined such that it gave the same value of  $T_g$  as that for TMDSC with a period of 120 s (and an average cooling rate of  $-0.3$  K/min), it has been shown (Hutchinson & Montserrat, 2001; Montserrat et al, 2005) that the magnitude of the temperature fluctuations increases the wider is the distribution of relaxation times (small  $\beta$ ) and the greater is the non-linearity of the relaxation kinetics (small  $x$ ), with interesting implications regarding the physical phenomena underlying the glass transition.

The effects of these material parameters,  $\beta$  and  $x$ , on the appearance of the TMDSC signals, such as those shown in Figure 5, are very different, as can be demonstrated rather simply by these Matlab simulations. In Figure 6 are shown the effects of changing  $x$  and  $\beta$  on the average heat capacity (Figures 6a and 6b, respectively) and on the complex heat capacity (Figures 6c and 6d, respectively).

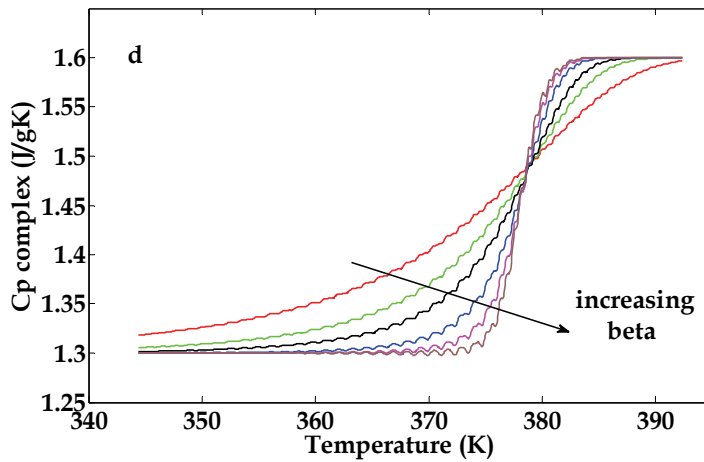
With respect to the average heat capacity signals in Figures 6a and 6b, the effects of increasing  $x$  and of increasing  $\beta$  are very similar: in both cases the transition broadens as the parameter value decreases towards zero. In respect of  $x$ , this is explained by the response becoming more non-linear as  $x$  decreases, giving rise to a greater relative dependence on the fictive temperature (cf. Equation 3), which means that the relaxation time shortens and the transition occurs at ever lower temperatures, observed in Figure 6a as a shift, for example, of



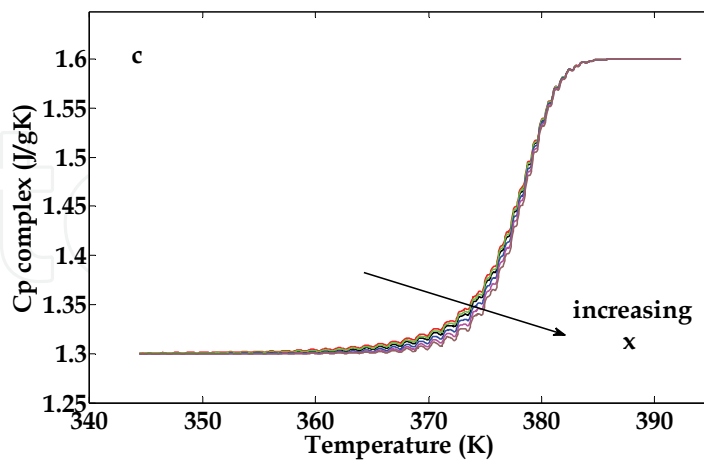
(a)



(b)



(c)



(d)

Fig. 6. Effects of  $x$  and  $\beta$  on the average and complex heat capacities in TMDSC on cooling through the glass transition region: (a) and (c)  $x=0.2, 0.3, 0.4, 0.6, 0.8, 1.0$ , with  $\beta=0.6$ ; (b) and (d)  $\beta=0.2, 0.3, 0.4, 0.6, 0.8, 1.0$ , with  $x=0.4$ . Other parameters:  $q_{av}=-3$  K/min,  $p=24$  s,  $A_T=0.5$  K,  $\Delta h^*/R=85$  kK

the mid-point temperature. In respect of  $\beta$ , reducing its value leads to a broadening of the distribution function (cf. Equation 5), with a consequent broadening of the response on cooling. In contrast, with respect to the complex heat capacity signals in Figures 6c and 6d, the effects of increasing  $x$  and of increasing  $\beta$  are very different: in one case (effect of  $x$ ) the transition remains essentially unaffected, whereas in the other case (effect of  $\beta$ ) the transition broadens as the parameter value decreases. In respect of  $x$ , this is explained by the fact that, in principle and as explained earlier, the dynamic transition occurs in equilibrium, where there is no effect of non-linearity since  $T_f = T$  (cf. Equation 3). The small amount of deviation observed in Figure 6c from a unique curve for all values of  $x$  may be explained by the overlapping of the dynamic and thermal transitions, which results in the system's not remaining truly in equilibrium in the latter part of the relaxation. In respect of  $\beta$ , on the other hand, even in equilibrium the effect of the width of the distribution will be evident. Indeed, the breadth of the relaxation in the complex heat capacity is a function only of  $\beta$ , since it is essentially independent of  $x$ , which means that such curves can be used for the independent experimental determination of the parameter  $\beta$  (Montserrat & Hutchinson, 2002). It is interesting also to note another characteristic feature of these curves, namely the appearance of ripples. These arise from the way in which the Fourier Transformation is made, in a window of a single cycle of the modulations, sliding this window along the time scale to cover the whole of the transition. In Figure 5, the window is slid by one whole cycle between Fourier Transformations, and hence the ripples do not appear. In Figure 6, the window is slid by the time step of the calculations, and hence the ripples do appear (Hutchinson & Montserrat, 1997). In the transition interval, the frequency of these ripples is twice the frequency of the heating rate modulations. In the experimental data these ripples should also appear, and indeed do so in the output signals from ADSC from Mettler Toledo, and their frequency is in agreement with the model predictions. These ripples do not appear in the output data from TMDSC equipment from other manufacturers, either because the data have been smoothed or because the Fourier Transformation window is slid along the time scale by integral cycles.

As a final comment on the use of TMDSC for the study of the glass transition in polymers, it is worth pointing out the relatively recent development of a multi-frequency technique, named TOPEM<sup>®</sup>, from Mettler Toledo. In this technique, instead of a periodic modulation of the temperature or of the heating rate as in TMDSC, the sample is subjected to a stochastic series of small temperature pulses, alternately positive and negative, with a user-defined range for the interval of time between these pulses, known as the switching time range. The combination of these two features, the stochastic nature and the use of pulses rather than modulations, allows an analysis of the frequency dependence to be made in a single scan, thus offering a significant advantage over TMDSC techniques which use only a single frequency in any one experiment. This advantage will become particularly apparent in the next section of this paper where the crosslinking reactions of thermosetting polymers are investigated. The method of analysis in TOPEM<sup>®</sup> is also different, using Laplace Transformation rather than Fourier Transformation, and is made in a Matlab environment using a Parameter Estimation Method (PEM). Amongst other output quantities, TOPEM<sup>®</sup> calculates what is called the quasi-static heat capacity,  $C_{p0}$ , which is the equivalent of the complex heat capacity of TMDSC, but for the limiting case of zero frequency. It is this quasi-static heat capacity which is first obtained from the experimental stochastic data, and is then separated into its frequency components. In a study of this technique applied to the glass transition of polymers (Fraga et al, 2007), the effects of a number of experimental parameters

were investigated, including the range of frequencies over which the technique could usefully be applied.

## 5. Crosslinking reaction in thermosetting polymers

In the crosslinking (or cure) process for thermosetting polymers, a chemical reaction takes place between the resin and the crosslinking agent (hardener) such that the monomers of the un-reacted resin are incorporated into a three-dimensional rigid network structure. In this process, the viscous liquid resin, which has a very low  $T_g$ , usually sub-ambient, is transformed into a stiff and hard material, with a high  $T_g$  and with numerous industrial applications, from surface coatings to the matrix material for high performance fibre reinforced composites. Usually, a stoichiometric ratio of resin to hardener will be used, as this gives the optimum properties of the cured material, including a maximum value of the glass transition temperature. In addition, though, the conditions under which the cure reaction is conducted can also be important: for example, the cure may be isothermal, and the isothermal cure temperature may be selected within quite a wide range, or the cure may be non-isothermal, at a constant heating rate over a temperature range, with various possibilities for the heating rate. The selection of cure conditions can be important. For instance, in isothermal cure at low temperatures, the increase in  $T_g$  of the system that results from the crosslinking reaction can be such that it becomes higher than the isothermal cure temperature. Under these conditions, vitrification will occur, since the partially cured material will then be at a temperature below its  $T_g$ . Vitrification, followed by devitrification, can also occur under some circumstance during non-isothermal cure. When a crosslinking system vitrifies, the reaction rate changes dramatically, from a relatively rapid rate, controlled by the chemical rate constants of the reaction, to a much slower rate, which is controlled by the rate of diffusion of the reacting species. The ability to predict whether or not vitrification will occur under any given cure conditions is of some importance, and hence it is necessary to describe the kinetics of the reaction.

A particularly good illustration of the importance of understanding the cure kinetics is afforded by the cure reaction that takes place during the fabrication of epoxy-clay nanocomposites. These materials consist of a small proportion, typically less than 5 wt%, of organically modified clay in an epoxy resin matrix. The structure of the clay is laminar, and the fundamental idea is that the clay layers should separate completely (exfoliate) and be distributed uniformly throughout the epoxy matrix in the final cured nanocomposite: in this way, the nanoclay provides a very efficient reinforcement because of its large surface area, and thus can strengthen and stiffen the epoxy without significantly increasing its density, of particular importance for aeronautical applications, for example. However, to obtain an exfoliated structure is difficult, because it depends on the relative rates of cure of the resin in the intra-gallery and extra-gallery regions of the clay. Control of these rates, i.e. of the kinetics of the reaction, is therefore of crucial importance in obtaining an optimised nanostructure of these materials (Montserrat et al, 2008; Pustkova et al, 2009). The following sections discuss how the cure kinetics can be simulated using Matlab, to model both conventional and Temperature Modulated DSC experiments.

### 5.1 Theoretical aspects of cure kinetics

In the absence of vitrification, the cure reaction is chemically controlled and the time dependence of the degree of cure, which is denoted by  $\alpha$  and which increases from 0

initially to 1 for the fully cured material, can be described by various different kinetic equations. One of the most widely used equations is that of Kamal (Kamal, 1974), which describes an autocatalytic reaction:

$$\left(\frac{d\alpha}{dt}\right)_{\text{chem}} = (k_1 + k_2\alpha^m)(1-\alpha)^n \quad (10)$$

where  $k_1$  and  $k_2$  are temperature dependent rate constants and the exponents  $m$  and  $n$  are the reaction orders. The rate constants depend on temperature according to the Arrhenius equation:

$$k_{c,1} = A_1 \exp\left(-\frac{E_{c,1}}{RT}\right) \quad (11a)$$

$$k_{c,2} = A_2 \exp\left(-\frac{E_{c,2}}{RT}\right) \quad (11b)$$

where  $A_1$  and  $A_2$  are pre-exponential constants,  $E$  is the activation energy, and  $R$  is the universal gas constant. In this equation, a subscript  $c$  has been added for  $k$  and  $E$  to indicate that these are values for the chemically controlled reaction.

These Equations 10 and 11 are sufficient to describe the kinetics of the cure reaction when it is chemically controlled, in other words in the absence of vitrification (to be discussed in detail below), and the predictions of this model can be compared with experimental DSC data in the form of heat flow as a function of time (for isothermal cure) or as a function of temperature (for non-isothermal cure). The specific heat flow,  $HF$  [W/g] is given by:

$$HF = \Delta H_{\infty} \frac{d\alpha}{dt} \quad (12)$$

where  $\Delta H_{\infty}$  is the total heat of reaction per unit mass [J/g] for a fully cured system. Typical results which emerge from this model are shown in Figures 7a and 7b for isothermal and non-isothermal cure, respectively, where the effects of some of the experimental parameters are included: in Figure 7a, four different isothermal cure temperatures (50°C, 60°C, 70°C and 80°C) are used, with the reaction occurring at shorter times as the cure temperature increases; in Figure 7b, four different heating rates are used (1, 2, 5 and 10 K/min), with the reaction shifting to higher temperatures with increasing heating rate.

By fitting these kinetic equations to the experimental data, it is possible to evaluate the various kinetic parameters, in particular the activation energies, the pre-exponential parameters, and the reaction exponents,  $m$  and  $n$ . In principle, the same parameter values will be obtained from both isothermal and non-isothermal experimental data. In practice, however, the kinetic equations are only an approximation to the real situation, which is generally much more complex, involving not just one reaction, for example the reaction of the primary amine of the cross-linking agent with the epoxy monomers, but also other reactions such as the reaction of secondary amines which result from the first reaction, and a homopolymerization reaction (etherification) which can be catalyzed by the tertiary amines resulting from the second reaction (Fernández-Francos et al, 2007; Kubisa & Penczek, 1999; Montserrat et al, 2008; Pascault et al, 2002; Tanaka & Bauer, 1988). The result of this added

complexity is that a best fit to non-isothermal data does not always result in a best fit for the isothermal data. Nevertheless, in most instances a satisfactory fit can be obtained to all the experimental data, and the evaluation of the parameter values then provides useful information about the reaction kinetics.

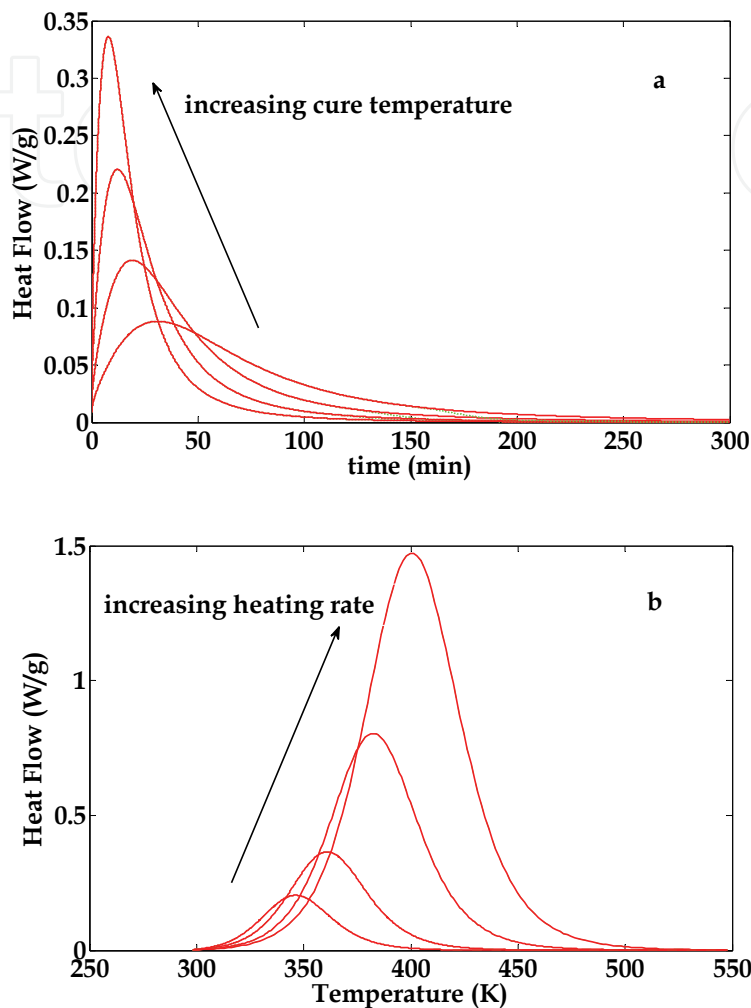


Fig. 7. Cure simulations under isothermal [(a): at 50°C, 60°C, 70°C and 80°C] and non-isothermal [(b): at 1, 2, 5 and 10 K/min] conditions. Parameters:  $m=0.5$ ,  $n=1.5$ ,  $A_1=10^{3.6}$  s,  $A_2=10^{3.4}$  s,  $E_{c,1}=51.8$  kJ/mol,  $E_{c,2}=41.5$  kJ/mol,  $\Delta H_{\infty}=520$  J/g

The usual procedure for evaluating the parameter values from the experimental data is first to determine the total heat of reaction, per unit mass of sample, from the non-isothermal cure curves. This is calculated as the area under the cure curve of heat flow per unit mass of sample as a function of temperature, normalized by the heating rate. For a stoichiometric ratio of diglycidyl ether of bisphenol-A (DGEBA) epoxy resin and a diamine curing agent, for example, this is approximately 400 J/g. The reason for using the non-isothermal cure rather than the isothermal cure is that in isothermal cure it is possible that vitrification might occur. If this happens, then the cure does not proceed to completion, but the cure rate decreases to zero before the reaction is complete, and it is not possible to identify, by conventional DSC, whether or not this occurs. An analysis of the isothermal cure curve under these circumstances, using the kinetic Equations 10-12 above, would lead to

erroneous results. In fact, it is also possible for vitrification to occur during non-isothermal cure, though the experimental circumstances for this (essentially, a very slow heating rate) are generally not those that are used in practice. The way in which the problem of vitrification during cure can be addressed by means of TMDSC is discussed in the following sections, first in a general way and then, separately, with respect to isothermal cure and non-isothermal cure. In these latter cases it will be shown how Matlab simulations of the cure under TMDSC conditions provide a rational way of interpreting the experimental results, and allow a comparison with other dynamic techniques operating over a quite different frequency range. The graphical representation aspects are particularly helpful.

## 5.2 Cure reaction with vitrification

Vitrification occurs, either in isothermal cure or in non-isothermal cure, when the glass transition temperature of the cross-linking system, which is continuously increasing as the degree of cross-linking increases, reaches and then exceeds the cure temperature. In isothermal cure, vitrification results in a rather rapid decrease in the rate of cure, as the rate of reaction changes from being controlled by the chemical rate constants,  $k_{c,1}$  and  $k_{c,2}$ , to being controlled by the diffusion of the reacting species, with a much slower rate determined by a diffusion rate constant,  $k_d$ . As a consequence, the reaction effectively stops, and the system remains only partially cured. Likewise, in non-isothermal cure, it is possible for the glass transition of the curing system to increase beyond the instantaneous value of the (continually increasing) cure temperature, generally provided that the rate of heating is sufficiently slow. The system therefore vitrifies, but, in contrast to isothermal cure, the cure temperature continues to increase at the imposed rate, and so the system will eventually devitrify when the cure temperature again exceeds the glass transition temperature of the system. In the simulation of cure with vitrification, therefore, there are two important aspects to consider: first, the dependence of the glass transition temperature of the curing system on the degree of cure, and second, the expression for the diffusion rate constant, and its dependence on temperature.

The relationship between the degree of cure,  $\alpha$ , and the glass transition temperature,  $T_g$ , of the curing system can be described by the DiBenedetto equation (DiBenedetto, 1987; Pascault & Williams, 1990):

$$\frac{T_g - T_{g0}}{T_{g\infty} - T_{g0}} = \frac{\lambda \alpha}{1 - (1 - \lambda)\alpha} \quad (13)$$

in which  $T_{g0}$  and  $T_{g\infty}$  are the glass transition temperatures of the uncured ( $\alpha=0$ ) and of the fully cured ( $\alpha=1$ ) system, respectively, and  $\lambda$  is a fitting parameter related to the ratio of the heat capacities of the fully cured and of the uncured system.

There have been a number of different expressions proposed for the diffusion rate constant and its dependence on temperature, and a summary of these has been presented earlier (Fraga et al, 2008). The expression that is perhaps most widely used, and the one that is used here, assumes a WLF temperature dependence (Williams et al, 1955; Wise et al, 1997):

$$k_d = k_{dg} \exp \left[ \frac{C_1(T - T_g)}{C_2 + T - T_g} \right] \quad (14)$$

where  $k_{dg}$  is the value of  $k_d$  when  $T_g$  is equal to the cure temperature, in other words at vitrification, and  $C_1$  and  $C_2$  are constants of the WLF equation, and are here taken to have their “universal” values of 40.2 and 51.6 K, respectively. As regards the value of  $k_{dg}$  for these simulations, there is a surprisingly large variation of values that are used in the literature; here we adopt the value of  $0.0051 \text{ s}^{-1}$  used in earlier work (Fraga et al, 2008).

The chemical rate constants,  $k_{c1}$  and  $k_{c2}$ , can be combined with the diffusion rate constant,  $k_d$ , to give overall rate constants,  $k_{tot,1}$  and  $k_{tot,2}$ , for the reaction, according to the Rabinowitch equation (Rabinowitch, 1937):

$$\frac{1}{k_{tot,1}} = \frac{1}{k_d} + \frac{1}{k_{c,1}} \quad (15a)$$

$$\frac{1}{k_{tot,2}} = \frac{1}{k_d} + \frac{1}{k_{c,2}} \quad (15b)$$

These overall rate constants are used in place of the rate constants  $k_1$  and  $k_2$  of the Kamal equation, Equation 10, in order to describe the cure rate during either isothermal or non-isothermal cure, including that part in which vitrification occurs. This set of Equations 10-15 is solved using Matlab in order to simulate the cure of these reacting systems under isothermal and non-isothermal conditions, which are considered separately in the following sections. In particular, the vitrification time is determined as a function of the experimental conditions, being defined as the time at which the glass transition temperature of the reacting system becomes equal to the cure temperature.

### 5.2.1 Isothermal cure with vitrification

As mentioned above, it is not possible by conventional DSC to identify, directly from the cure curve, when vitrification occurs for a given isothermal cure temperature,  $T_c$ . To determine the vitrification time, it is necessary to repeat the isothermal cure for a series of different cure times, with a second (non-isothermal) scan after each isotherm in order to determine the glass transition temperature corresponding to each isothermal cure time. A plot of  $T_g$  as a function of cure time then allows the vitrification time,  $t_v$ , to be found as the cure time for which  $T_g = T_c$ . This procedure has been used in the past (Montserrat, 1992), but it is impractical on account of the length of time involved in making numerous repeated isothermal cure experiments. It is in this respect that TMDSC offers an important advantage: the reversing or complex heat capacity signal is responsive to the changes that take place when the system vitrifies, in just the same way as these signals respond to a glass transition on cooling, and hence at the time of vitrification in isothermal cure the complex heat capacity shows a sigmoidal change from a liquid-like to a glassy value. By TMDSC, therefore, it is possible to identify the vitrification time directly from the isothermal cure curve, and it is conventionally taken to be at the mid-point of the sigmoid.

This approach has been adopted successfully by a number of workers (Alig et al, 1999; Lange et al, 2000; Montserrat & Cima, 1999; Montserrat & Martin, 2002; Van Assche et al, 1998). Nevertheless, it raises the question of how this measurement of the vitrification time, which depends on the frequency of modulation, can be reconciled with that obtained by the lengthy conventional DSC procedure, which does not depend on the frequency. Clearly this leads again to the relationship between the frequency dependence and the rate dependence of  $T_g$ , which has been discussed above. In the present instance, the effect of frequency can be

demonstrated very clearly by means of Matlab simulations, and this approach transpires to be illuminating also about the study of vitrification by other techniques, such as Dielectric Analysis (DEA), which operate at much higher frequencies. The starting point for these simulations is that vitrification occurs when the glass transition temperature of the curing system, which increases with increasing frequency, reaches the cure temperature. However, rather than use this as the criterion for defining vitrification, we adopt here instead an alternative and simpler procedure, which is to assign a frequency dependence to the cure temperature, such that it *decreases* with increasing frequency according to the following equation (Fraga et al, 2008a):

$$\ln\left(\frac{f}{f_r}\right) = \frac{E_f}{R} \left( \frac{1}{T_c(f)} - \frac{1}{T_c} \right) \quad (16)$$

In this equation,  $E_f$  is the activation energy controlling the frequency dependence of  $T_c$  (equivalent to the activation energy for  $T_g$ ), and  $f_r$  is a reference frequency for which the dynamic cure temperature,  $T_c(f)$ , is considered to be equal to the cure temperature,  $T_c$ . Since the vitrification time determined by conventional DSC makes use of a glass transition temperature determined on heating after cooling freely, the correspondence between cooling rate and frequency (Donth et al, 1997; Hensel & Schick, 1998; Hutchinson, 1998; Montserrat, 2000; Weyer et al, 1997) allows us to assign a value of  $1/60 \text{ s}^{-1}$  for the reference frequency. The results of such a simulation are shown in Figure 8, which shows the increase of  $T_g$  of the curing system as a function of isothermal cure time.

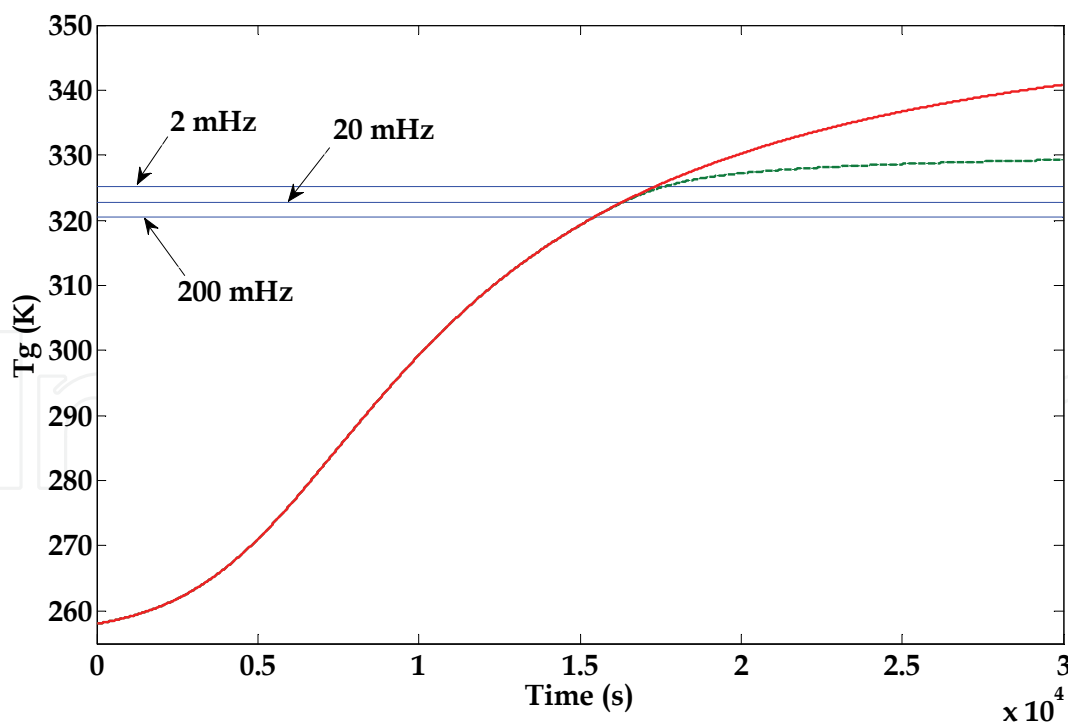


Fig. 8. Simulation of isothermal cure: chemical reaction without vitrification (full line, red curve); with vitrification (dashed line, green curve). Horizontal blue lines indicate frequency dependent isothermal cure temperature: 2 mHz (upper); 20 mHz (middle); 200 mHz (lower). Parameter values:  $m=1$ ,  $n=2$ ,  $\lambda=0.5$ ,  $E_f/R=100 \text{ kK}$ ,  $T_{g0}=-15^\circ\text{C}$ ,  $T_{g\infty}=85^\circ\text{C}$ ,  $T_c=50^\circ\text{C}$

In the absence of vitrification, the  $T_g$  of the curing system increases from its value,  $T_{g0}$ , for the un-reacted resin monomer to a final value,  $T_{g\infty}$ , for the fully reacted system, as shown by the full line in Figure 8, though this final value is not reached within the time scale shown. On the other hand, if vitrification intervenes then the rate of cure will reduce dramatically and the system will not reach a full cure, as shown by the dashed line. The vitrification time,  $t_v$ , is determined as the time at which the  $T_g$  of the curing system becomes equal to the cure temperature,  $T_c$ . Since the cure temperature has been assigned a frequency dependence, this means that  $t_v$  will also depend on the frequency, and in a way this is clearly non-linear. It is a straightforward matter to evaluate  $t_v$  for a range of frequencies from such simulations, for a given isothermal cure temperature, and a typical result is shown in Figure 9.

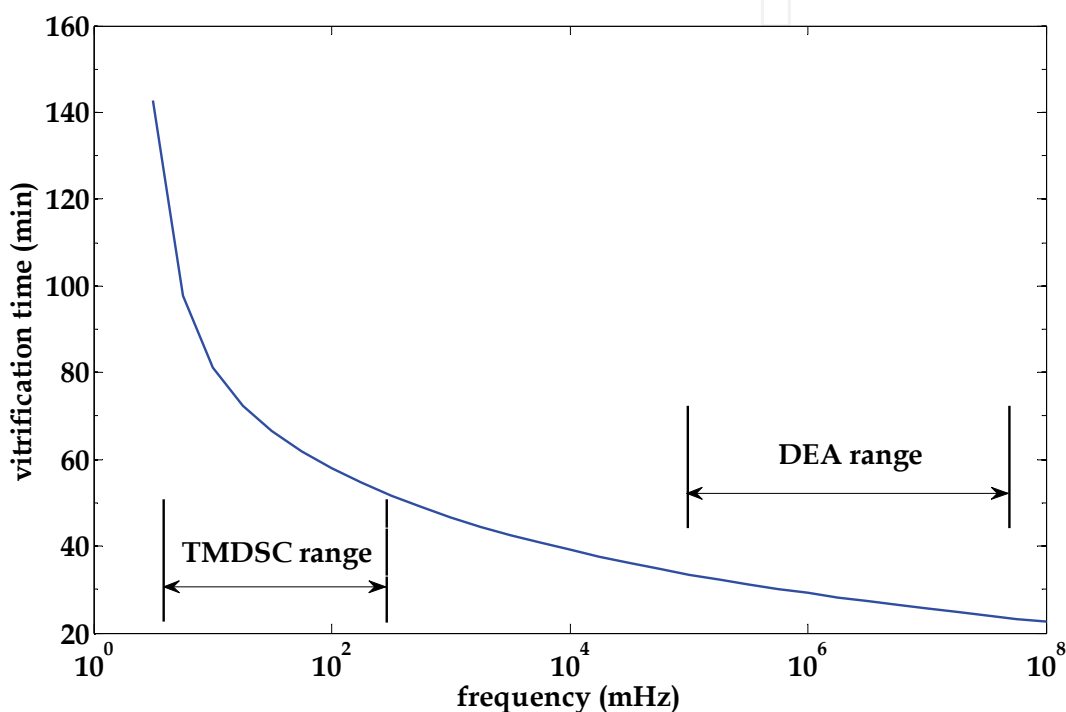


Fig. 9. Vitrification time as a function of frequency (on a logarithmic scale) for isothermal cure at 70°C with the following parameter values:  $m=0.23$ ,  $n=1.43$ ,  $\lambda=0.66$ ,  $E_f/R=50$  kK

As has been shown elsewhere (Fraga et al, 2008a), in a more extensive simulation covering a range of isothermal curing temperatures and examining the effects of various parameter values, such results are in excellent agreement with experimental data. In particular, the important feature of Figure 9 is that, at low frequencies, in the typical range available by TMDSC, there is a marked upward curvature, whereas at high frequencies, typical of those available in DEA, there is a good linear relationship between  $t_v$  and the logarithm of the frequency. The data obtained by TMDSC experiments are subject to a significant experimental error in view of the fact that this technique operates at only a single frequency; this means that a new sample must be prepared for each different frequency, which inevitably introduces some small variation in the resin to hardener ratio, which has a consequent effect on the cure kinetics. Nevertheless, it is possible to identify the upward curvature in the dependence of  $t_v$  on  $\log(f)$  at low frequency from a close observation of some light-heating TMDSC experiments (Fraga et al, 2008a; Van Assche et al, 2001). In addition, the more recent technique of TOPEM<sup>®</sup>, a TMDSC technique which allows a range of frequencies to be

studied in a single scan, shows this upward curvature even more clearly (Fraga et al, 2008b). On the other hand, at high frequencies the linear dependence of  $t_v$  on  $\log(f)$  has been known for some time (Alig et al, 1999; Fournier et al, 1996; Mangion & Johari, 1990; Montserrat et al, 2003). Not only do these Matlab simulations describe very well the data at both low and high frequencies, but they also resolve the observation made by Montserrat et al (Montserrat et al, 2003) that the extrapolation of the  $t_v$  data from the high frequencies corresponding to DEA results did not coincide with the data at low frequencies corresponding to TMDSC data: it is clear from Figure 9 that this is simply because of the upward curvature in this representation. In fact, in DEA experiments it is not really the vitrification time, in the sense of a change from a chemical controlled to a diffusion controlled kinetics, that is being determined; rather it is the dynamic  $\alpha$ -relaxation, for which the temperature of the relaxation peak is equal to the cure temperature at what might be called a dynamic vitrification time. This is clear from Figure 8, where at high frequencies the location of the dynamic vitrification time occurs well before the bifurcation which represents the change in kinetics of the reaction.

### 5.2.2 Non-isothermal cure with vitrification and devitrification

For the simulation of non-isothermal cure with vitrification (and devitrification), the same set of Equations 10 to 15 is solved using Matlab, and the same procedure is adopted of assigning a frequency dependence to the cure temperature according to Equation 16. If the heating rate is sufficiently slow, then the  $T_g$  of the reacting system can surpass the cure temperature, and vitrification will occur. This dramatically reduces the rate of reaction, and hence  $T_g$  increases only little while the cure temperature continuously increases according to the imposed rate of heating. Consequently, a point is reached where the cure temperature again exceeds the glass transition temperature, and the sample devitrifies and proceeds to a full cure. By conventional DSC these subtle changes in the rate of cure cannot be identified. On the other hand, by TMDSC the changes in the complex heat capacity allow both vitrification and devitrification to be identified, as a sigmoidal decrease and increase, respectively, in  $C_p^*$ , with their separation being greater the slower is the heating rate (Fraga et al, 2010a, 2010b). Generally, the heating rates need to be very slow in order to observe these phenomena: with an epoxy-amine system, for example, these rates are from 0.05 to 0.015 K/min. Furthermore, with TOPEM<sup>®</sup> the frequency dependence of vitrification and devitrification can be found experimentally, and Matlab simulations provide excellent agreement with the experimental observations.

Figure 10 shows an illustration of non-isothermal cure and the effect of a frequency dependent cure temperature. Here it can be seen that vitrification occurs at a temperature of about 310 K, depending on the frequency of modulation, and that shortly thereafter the cure rate decreases significantly. The rapidity with which the cure rate decreases and the extent to which the cure continues after the glass transition temperature reaches the cure temperature are dictated by the magnitude of the diffusion rate constant  $k_{dg}$  in Equation 14. As mentioned earlier, there is a surprisingly large variation in values assigned to this parameter in the literature, when one might have expected it to have approximately the same value for any vitrifying system, given that the glass transition is a universal phenomenon with a timescale that is conventionally taken to be around 100 seconds. Nevertheless, values for  $k_{dg}$  as different as  $4 \times 10^{-5} \text{ s}^{-1}$  and  $100 \text{ s}^{-1}$  can be found in the literature (Fraga et al, 2008a). This remains an area for further investigation.

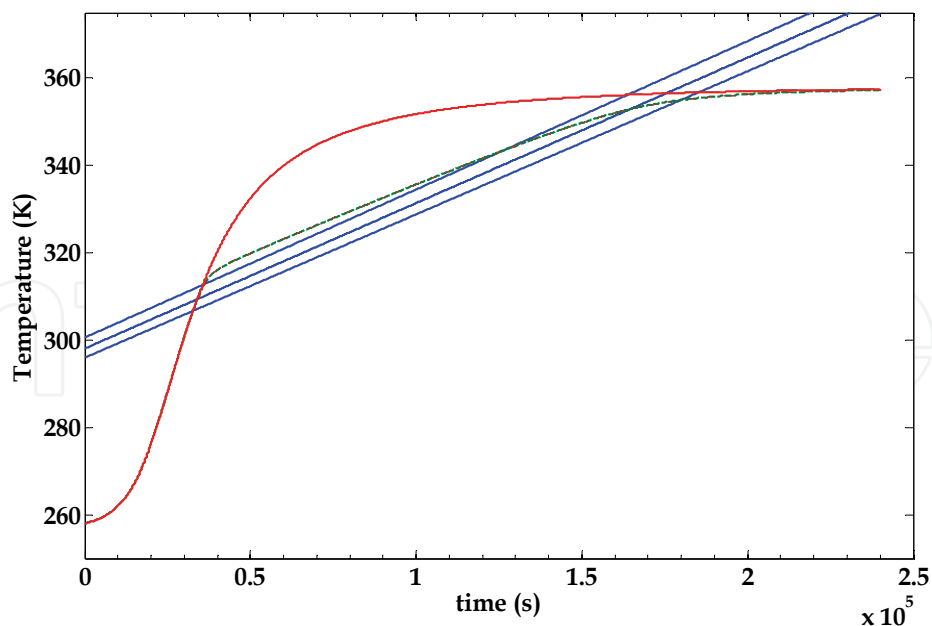


Fig. 10. Simulation of non-isothermal cure, showing variation of  $T_g$  during cure without vitrification (red full curve) and with vitrification and devitrification (green dashed curve). As there is now space available, following the format change, this caption could include the experimental conditions, which are: heating rate=0.02 K/min,  $m=1$ ,  $n=2$ ,  $\lambda=0.5$ ,  $E_t/R=100$  kK,  $T_{g0}=-15^\circ\text{C}$ ,  $T_{g\infty}=85^\circ\text{C}$

Following vitrification, the cure temperature continues to increase at the experimentally imposed rate, and consequently the system will devitrify when the cure temperature again exceeds the glass transition temperature. This generally occurs when the glass transition temperature is approaching its value for the fully cured system,  $T_{g\infty}$ . In Figure 10 this is seen as the crossing point of the cure curve and the heating rate curve, which is located in the region of the cure curve which is almost horizontal. The temperature at which devitrification occurs is therefore a good approximation to that of the fully cured system, and is almost independent of frequency (Fraga et al, 2010a; Fraga et al, 2010b). This is an important observation, as can be illustrated by a good example. The tri-functional epoxy resin, tri-glycidyl para-amino phenol (TGAP), when cured with diamino diphenyl sulphone (DDS), results in a very highly cross-linked network structure. In fact, the cross-link density is so high that the glass transition cannot be identified by DSC or TMDSC for this system, and it is common practice to determine the  $T_g$  instead by other techniques, for example by dynamic mechanical analysis (DMA) (Frigione & Calò, 2008). This is clearly not an ideal situation for studying the kinetics of cure and its effects on the structure and properties of the cured system: for instance, DMA does not measure the same  $T_g$  as for DSC or TMDSC, and operates at a higher frequency than does TMDSC (Hutchinson, 2010). However, by curing non-isothermally at a very slow rate, it is possible to identify both vitrification and devitrification in this system, with the temperature at which devitrification occurs being clearly defined, thus allowing the calorimetric determination of  $T_{g\infty}$ .

## 6. Conclusions

This paper summarises some aspects of the glass transition of polymers that have been investigated by means of simulations made in the Matlab environment. These aspects have

included the following. First, the basic glass transformation process, involving cooling from an equilibrium melt to a non-equilibrium glass state, has been simulated by Matlab to show, in particular, the cooling rate dependence of the glass transition temperature and the endothermic peak that occurs in the heat flow, as measured by DSC, on reheating after annealing at a temperature within the glassy state. These simulations required the solution of a system of differential equations using the "ode" routines. The use of such simulations in which the effects of both experimental and material parameters were investigated led to a method (the peak shift method) for the determination of one of the material parameters, the non-linearity parameter,  $x$ .

Second, the technique of Temperature Modulated DSC was simulated by Matlab in order to better interpret the various new signals that this technique gives in addition to those available by conventional DSC. These simulations made use of "fft" routines in order to evaluate the average values and amplitudes of the periodically varying heating rate and heat flow signals. Again, these simulations were made so as to investigate the effects of both the experimental and the material parameters, and the results led to a clear interpretation of the complex heat capacity and its dependence on these parameters. Among other results, this approach allowed the clear distinction to be made between the thermal and dynamic glass transition temperatures, and led to an interpretation of the relationship between them in respect of the correspondence between cooling rate and frequency. Such simulations also led to a new method for the experimental determination of the other material parameter, the non-exponentiality parameter  $\beta$ .

Third, the processes of vitrification and devitrification that occur in thermosetting systems have been investigated by using Matlab to simulate the cure reaction in both isothermal and non-isothermal conditions. In particular, as regards isothermal cure, the effects of frequency have been simulated, and have allowed some hitherto apparently anomalous aspects of the frequency dependence of the vitrification time over a wide range of frequencies to be explained. With respect to non-isothermal cure, it has been shown that the devitrification process occurs at a temperature very close to the glass transition temperature of the fully cured system, and therefore provides a means of determining  $T_{g\infty}$  calorimetrically for systems in which this is otherwise not possible. In the analysis and simulation of these processes, the graphical representation capabilities of Matlab were particularly useful.

## 7. Acknowledgement

This work was supported by a grant from the Spanish Ministry of Education and Science, Project MAT 2008-06284-C03-03.

## 8. References

- Adam, G. & Gibbs, J.H. (1965). On Temperature Dependence of Cooperative Relaxation Properties in Glass-forming Liquids. *J. Chem. Phys.* Vol.43, Iss.1, pp. 139-146, ISSN 0021-9606
- Alig, I.; Jenninger, W. & Schawe, J.E.K. (1999). Curing Kinetics of Phase Separating Thermosets Studied by DSC, TMDSC and Dielectric Relaxation Spectroscopy. *Thermochim. Acta*, Vol.330, Iss.1-2, pp. 167-174, ISSN 0040-6031
- Berens, A.R. & Hodge, I.M. (1982). Effects of Annealing and Prior History on Enthalpy Relaxation in Glassy Polymers. I. Experimental Study on Poly(vinyl chloride). *Macromolecules*, Vol.15, Iss.3, pp. 756-761, ISSN 0024-9297

- DiBenedetto, A.T. (1987). Prediction of the Glass-Transition Temperature of Polymers - a Model Based on the Principle of Corresponding States. *J. Polym. Sci. Part B. Polym. Phys.*, Vol.25, Iss.9, pp. 1949-1969, ISSN 0887-6266
- Donth, E.; Korus, J.; Hempel, E. & Beiner, M. (1997). Comparison of DSC Heating Rate and HCS Frequency at the Glass Transition. *Thermochim. Acta*, Vol.305, Iss.Nov, pp. 239-249, ISSN 0040-6031
- Fernández-Francos, X.; Salla, J.M.; Cadenato, A.; Morancho, J.M.; Mantecón, A.; Serra, A. & Ramis, X. (2007). Influence of the Initiating Mechanism on the Cationic Photopolymerization of a Cycloaliphatic Epoxy Resin with Arylsulfonium Salts. *J. Polym. Sci. Part A: Polym. Chem.*, Vol.45, Iss.1, pp. 16-25, ISSN 0887-624X
- Fournier, J.; Williams, G.; Duch, C. & Aldridge, G.A. (1996). Changes in Molecular Dynamics during Bulk Polymerization of an Epoxide-Amine System as Studied by Dielectric Relaxation Spectroscopy. *Macromolecules*, Vol.29, Iss.22, pp.7097-7107, ISSN 0024-9297
- Fraga, I.; Hutchinson, J.M. & Montserrat, S. (2010a). Vitrification and Devitrification during the Non-Isothermal Cure of a Thermoset. *J. Thermal Anal. Calorim.*, Vol.99, Iss.3, pp. 925-929, ISSN 1388-6150
- Fraga, I.; Montserrat, S. & Hutchinson, J.M. (2007). TOPEM, a New Temperature Modulated DSC Technique - Application to the Glass Transition of Polymers. *J. Thermal Anal. Calorim.*, Vol.87, Iss.1, pp. 119-124, ISSN 1418-2874
- Fraga, I.; Montserrat, S. & Hutchinson, J.M. (2008a). Vitrification during the Isothermal Cure of Thermosets: Comparison of Theoretical Simulations with Temperature-Modulated DSC and Dielectric Analysis. *Macromol. Chem. Phys.*, Vol.209, Iss.19, pp. 2003-2011, ISSN 1022-1352
- Fraga, I.; Montserrat, S. & Hutchinson, J.M. (2008b). Vitrification during the Isothermal Cure of Thermosets. Part 1. An Investigation using TOPEM, a New Temperature Modulated Technique. *J. Thermal Anal. Calorim.*, Vol.91, Iss.3, pp. 687-695, ISSN 1388-6150
- Fraga, I.; Montserrat, S. & Hutchinson, J.M. (2010b). Vitrification and Devitrification during the Non-Isothermal Cure of a Thermoset. Theoretical Model and Comparison with Calorimetric Experiments. *Macromol. Chem. Phys.*, Vol.211, Iss.1, pp. 57-65, ISSN 1022-1352
- Frigione, M. & Calò, E. (2008). Influence of an Hyperbranched Aliphatic Polyester on the Cure Kinetic of a Trifunctional Epoxy Resin. *J. Appl. Polymer Sci.*, Vol.107, Iss.3, pp. 1744-1758, ISSN 0021-8995
- Gibbs, J.H. & DiMarzio, E.A. (1958). Nature of the Glass Transition and the Glassy State. *J. Chem. Phys.* Vol.28, Iss.3, pp. 373-383, ISSN 0021-9606
- Gill, P.S.; Sauerbrunn, S.R. & Reading M. (1993). Modulated Differential Scanning Calorimetry. *J. Thermal Anal.*, Vol.40, Iss.3, pp. 931-939, ISSN 0368-4466
- Hensel, A. & Schick, C. (1998). Relation between Freezing-in due to Linear Cooling and the Dynamic Glass Transition Temperature by Temperature-modulated DSC. *J. Non-Cryst. Sol.*, Vol.235, Iss.Aug, pp. 510-516, ISSN 0022-3093
- Hodge, I.M. (1994). Enthalpy Relaxation and Recovery in Amorphous Materials. *J. Non-Cryst. Sol.* Vol.169, Iss.3, pp. 211-266, ISSN 0022-3093

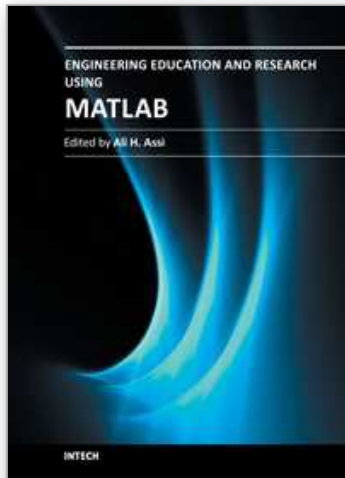
- Hutchinson, J.M. (1987). Thermal Cycling of Glasses: a Theoretical and Experimental Approach, In: *Molecular Dynamics and Relaxation Phenomena in Glasses*, Th. Dorfmüller & G. Williams, (Eds.), pp. 172-187, Springer-Verlag, ISBN 3-540-17801-5, Berlin
- Hutchinson, J.M. (1995). Physical Aging of Polymers. *Prog. Polym. Sci.*, Vol.20, Iss.4, pp. 703-760, ISSN 0079-6700
- Hutchinson, J.M. (1998). Characterising the Glass Transition and Relaxation Kinetics by Conventional and Temperature-modulated Differential Scanning Calorimetry. *Thermochim. Acta*, Vol.324, Iss.1-2, pp. 165-174, ISSN 0040-6031
- Hutchinson, J.M. (2010). Determination of the Glass Transition Temperature. *J. Thermal Anal. Calorim.*, Vol.98, Iss.3, pp. 579-589, ISSN 1388-6150
- Hutchinson, J.M. & Montserrat, S. (1997). A Theoretical Model of Temperature-Modulated Differential Scanning Calorimetry in the Glass Transition Region. *Thermochim. Acta*, Vol.305, Iss.Nov, pp. 257-265, ISSN 0040-6031
- Hutchinson, J.M. & Montserrat, S. (2001). The Application of Temperature-modulated DSC to the Glass Transition Region II. Effect of a Distribution of Relaxation Times. *Thermochim. Acta*, Vol.377, Iss.1-2, pp. 63-84, ISSN 0040-6031
- Hutchinson, J.M. & Ruddy, M. (1988). Thermal Cycling of Glasses. II. Experimental Evaluation of the Structure (or Non-linearity) Parameter  $x$ . *J. Polym. Sci. Polym. Phys. Ed*, Vol.26, Iss.11, pp. 2341-2366, ISSN 0887-6266
- Hutchinson, J.M. & Ruddy, M. (1990). Thermal Cycling of Glasses. III. Upper Peaks. *J. Polym. Sci. Polym. Phys. Ed*, Vol.28, Iss.11, pp. 2127-2163, ISSN 0887-6266
- Hutchinson, J.M. & Kovacs, A.J. (1976). A Simple Phenomenological Approach to the Thermal Behavior of Glasses during Uniform Heating or Cooling. *J. Polym. Sci. Polym. Phys. Ed*. Vol.14, Iss.9, pp. 1575-1590, ISSN 0887-6266
- Illers, K.H. (1969). Einfluss der Thermischen Vorgeschichte auf die Eigenschaften von Polyvinylchlorid. *Makromol. Chem.*, Vol.127, Iss.Sept, pp. 1-33, IDS E1355
- Jiang, X.; Hutchinson, J.M. & Imrie, C.T. (1998). Temperature-Modulated Differential Scanning Calorimetry. Part II. Determination of Activation Energies. *Polymer Int.*, Vol.47, Iss.1, pp. 72-75, ISSN 0959-8103
- Kamal, M.R. (1974). Thermoset Characterization for Moldability Analysis. *Polym. Eng. Sci.*, Vol.14, Iss.3, pp. 231-239, ISSN 0032-3888
- Kohlrausch, F. (1866). Beitrage zur Kenntnifs der Elastischen Nachwirkung. *Annalen der Physik und Chemie* Vol.128, No.5, pp. 1-20.
- Kovacs, A.J. (1963). Transition Vitreuse dans les Polymères Amorphes. Etude Phénoménologique. *Fortschr. Hochpolym. Forsch.*, Vol.3, pp. 394-507.
- Kovacs, A.J.; Aklonis, J.J.; Hutchinson, J.M. & Ramos, A.R. (1979). Isobaric Volume and Enthalpy Recovery of Glasses. II. A Transparent Multiparameter Theory. *J. Polym. Sci. Polym. Phys. Ed*. Vol.17, Iss.7, pp. 1097-1162, ISSN 0887-6266
- Kovacs, A.J. & Hutchinson, J.M. (1979). Isobaric Thermal Behavior of Glasses during Uniform Cooling and Heating: Dependence of the Characteristic Temperatures on the Relative Contributions of Temperature and Structure to the Rate of Recovery. II. A One-parameter Approach. *J. Polym. Sci. Polym. Phys. Ed*. Vol.17, Iss.12, pp. 2031-2058, ISSN 0887-6266

- Kubisa, P. & Penczek, S. (1999). Cationic Activated Monomer Polymerization of Heterocyclic Monomers. *Prog. Polym. Sci.*, Vol.24, Iss.10, pp. 1409-1437, ISSN 0079-6700
- Lange, J.; Altmann, N.; Kelly, C.T. & Halley, P.J. (2000). Understanding Vitrification during Cure of Epoxy Resins using Dynamic Scanning Calorimetry and Rheological Techniques. *Polymer*, Vol.41, Iss.15, pp. 5949-5955, ISSN 0032-3861
- Mangion, M.B.M. & Johari, G.P. (1990). Relaxations of Thermosets. 4. A Dielectric Study of Cross-Linking of Diglycidyl Ether of Bisphenol-A by 2 Curing Agents. *J. Polym. Sci.: Polym. Phys.*, Vol.28, Iss.9, pp. 1621-1639, ISSN 0887-6266
- Montserrat, S. (1992). Vitrification and Further Structural Relaxation in the Isothermal Curing of an Epoxy-Resin. *J. Appl. Polymer Sci.*, Vol.44, Iss.3, pp. 545-554, ISSN 0021-8995
- Montserrat, S. (2000). Measuring the Glass Transition of Thermosets by Alternating Differential Scanning Calorimetry. *J. Thermal Anal. Calorim.*, Vol.59, Iss.1-2, pp. 289-303, ISSN 1418-2874
- Montserrat, S.; Calventus, Y. & Hutchinson, J.M. (2005). Effect of Cooling Rate and Frequency on the Calorimetric Measurement of the Glass Transition. *Polymer*, Vol.46, Iss.26, pp. 12181-12189, ISSN 0032-3861
- Montserrat, S & Cima, I. (1999). Isothermal Curing of an Epoxy Resin by Alternating Differential Scanning Calorimetry. *Thermochim. Acta*, Vol.330, Iss.1-2, pp. 189-200, ISSN 0040-6031
- Montserrat, S. & Hutchinson, J.M. (2002). On the Measurement of the Width of the Distribution of Relaxation Times in Polymer Glasses. *Polymer*, Vol.43, Iss.2, pp. 351-355, ISSN 0032-3861
- Montserrat, S. & Martin, J.G. (2002). The Isothermal Curing of a Diepoxide-Cycloaliphatic Diamine Resin by Temperature Modulated Differential Scanning Calorimetry. *J. Appl. Polymer Sci.*, Vol.85, Iss.6, pp. 1263-1276, ISSN 0021-8995
- Montserrat, S.; Román, F. & Colomer, P. (2003). Vitrification and Dielectric Relaxation during the Isothermal Curing of an Epoxy-Amine Resin. *Polymer*, Vol.44, Iss.1, pp. 101-114, ISSN 0032-3861
- Montserrat, S.; Román, F.; Hutchinson, J.M. & Campos, L. (2008). Analysis of the Cure of Epoxy Based Layered Silicate Nanocomposites: Reaction Kinetics and Nanostructure Development. *J. Appl. Polymer Sci.*, Vol.108, Iss.2, pp. 923-938, ISSN 0021-8995
- Moynihan, C.T.; Eastal A.J.; DeBolt, M.A. & Tucker J. (1976). Dependence of Fictive Temperature of Glass on Cooling Rate. *J. Am. Ceram. Soc.* Vol.59, Iss.1-2, pp. 12-16, ISSN 0002-7820
- Narayanaswamy, O.S. (1971). Model of Structural Relaxation in Glass. *J. Am. Ceram. Soc.* Vol.54, Iss.10, pp. 491-198, ISSN 0002-7820
- Neki, N. & Geil P.H. (1973). Morphology-property Studies of Amorphous Polycarbonate. *J. Macromol. Sci. Phys.*, Vol.B8, Iss.1-2, pp. 295-341, ISSN 0022-2348
- Pappin, A.J.; Hutchinson, J.M. & Ingram, M.D. (1994). The Appearance of Annealing Pre-peaks in Inorganic Glasses: New Experimental Results and Theoretical Interpretation. *J. Non-Cryst. Sol.*, Vol.172, Part.1, pp. 584-591, ISSN 0022-3093
- Pascualt, J.-P.; Sautereau, H.; Verdu, J. & Williams, R.J.J. (2002). *Thermosetting Polymers*, Marcel Dekker, ISBN 0-8247-0670-6, New York

- Pascualt, J.-P. & Williams, R.J.J. (1990). Glass-Transition Temperature Versus Conversion Relationships for Thermosetting Polymers. *J. Polym. Sci. Part B. Polym. Phys.*, Vol.28, Iss.1, pp. 85-95, ISSN 0887-6266
- Pustkova, P.; Hutchinson, J.M.; Román, F. & Montserrat, S. (2009). Homopolymerization Effects in Polymer Layered Silicate Nanocomposites Based Upon Epoxy Resin: Implications for Exfoliation. *J. Appl. Polymer Sci.*, Vol.114, Iss.2, pp. 1040-1047, ISSN 0021-8995
- Rabinowitch, E. (1937). Collision, Co-ordination, Diffusion and Reaction Velocity in Condensed Systems. *Trans. Faraday Soc.*, Vol.33, Iss.2, pp. 1225-1232, ISSN 0014-7672
- Ramos, A.R.; Hutchinson, J.M. & Kovacs, A.J. (1984). Isobaric Thermal Behavior of Glasses during Uniform Cooling and Heating. III. Predictions from the Multiparameter KAHR Model. *J. Polym. Sci. Polym. Phys. Ed*, Vol.22, Iss.9, pp. 1655-1695, ISSN 0887-6266
- Reading, M.; Elliott, D. & Hill, V.L. (1993a). A New Approach to the Calorimetric Investigation of Physical and Chemical Transitions. *J. Thermal Anal.*, Vol.40, Iss.3, pp. 949-955, ISSN 0368-4466
- Reading, M.; Hahn, B.K. & Crowe, B.S. (1993b). Method and Apparatus for Modulated Differential Analysis. *United States Patent*, 5,224,775 (July 6, 1993)
- Retting, W. (1969). Zur Abhängigkeit der Mechanischen Eigenschaften von Thermoplasten von ihrer Thermischen Vorgeschichte. *Angewandte Makromol. Chem.*, Vol.8, Iss. Sept, pp. 87-98, ISSN 0003-3146
- Richardson, M.J. & Savill, N.G. Derivation of Accurate Glass-transition Temperatures by Differential Scanning Calorimetry. *Polymer*, Vol.16, Iss.10, pp. 753-757, ISSN 0032-3861
- Ruddy, M. & Hutchinson J.M. (1988). Multiple Peaks in Differential Scanning Calorimetry of Polymer Glasses. *Polym. Comm.*, Vol.29, Iss.5, pp. 132-134, ISSN 0263-6476
- Schawe, J.E.K. (1995). A Comparison of Different Evaluation Methods in Modulated Temperature DSC. *Thermochim. Acta*, Vol.260, Iss. Aug, pp. 1-16, ISSN 0040-6031
- Simon, F. (1931). Über den Zustand der Unterkühlten Flüssigkeiten und Gläser. *Z. anorg. Allgem. Chem.*, Vol.203, Iss.1/2, (December 1931), pp. 219-227, ISSN 0044-2313
- Tanaka, Y. & Bauer, R.S. (1988). Curing Reactions, In: *Epoxy Resins, Chemistry and Technology*, May, C.A. Ed., pp. 285-463, Marcel Dekker, ISBN 0-8247-7690-9, New York
- Tool, A.Q. (1946). Relation between Inelastic Deformability and Thermal Expansion of Glass in its Annealing Range. *J. Am. Ceram. Soc.*, Vol.29, Iss.9, pp. 240-253, ISSN 0002-7820
- Tool, A.Q. (1948). Effect of Heat-treatment on the Density and Constitution of High-silica Glasses of the Borosilicate Type. *J. Am. Ceram. Soc.*, Vol.31, Iss.7, pp. 177-186, ISSN 0002-7820
- Tool, A.Q. & Eichlin, C.G. (1931). Variations in the Heating Curves of Glass by Heat Treatment. *J. Am. Ceram. Soc.*, Vol.14, Iss.4, (April 1931), pp. 276-308, ISSN 0002-7820
- Van Assche, G.; Van Hemelrijck, A.; Rahier, H. & Van Mele, B. (1998). Modulated Temperature Differential Scanning Calorimetry: Cure, Vitrification, and Devitrification of Thermosetting Systems. *Thermochim. Acta*, Vol.305, Iss. Nov., pp. 317-334, ISSN 0040-6031

- Van Assche, G.; Van Mele, B. & Saruyama, Y. (2001). Frequency Dependent Heat Capacity in the Cure of Epoxy Resins. *Thermochim. Acta*, Vol.377, Iss.1-2, pp. 125-130, ISSN 0040-6031
- Weyer, S.; Hensel, A.; Korus, J.; Donth, E. & Schick, C. (1997). Broad Band Heat Capacity Spectroscopy in the Glass-transition Region of Polystyrene. *Thermochim. Acta*, Vol.305, Iss.Nov, pp. 251-255, ISSN 0040-6031
- Williams, G. & Watts, D.C. (1970). Non-symmetrical Dielectric Relaxation Behaviour Arising from a Simple Empirical Decay Function. *Trans. Faraday Soc.* Vol.66, Iss.565P, pp. 80-85, IDS F3962
- Williams, M.L.; Landel, R.F. & Ferry, J.D. (1955). Mechanical Properties of Substances of High Molecular Weight. 19. The Temperature Dependence of Relaxation Mechanisms in Amorphous Polymers and Other Glass-Forming Liquids. *J. Amer. Chem. Soc.*, Vol.77, Iss.14, pp. 3701-3707, ISSN 0002-7863
- Wise, C.W.; Cook, W.D. & Goodwin, A.A. (1997). Chemico-Diffusion Kinetics of Model Epoxy-Amine Resins. *Polymer*, Vol.38, Iss.13, pp. 3251-3261, ISSN 0032-3861

IntechOpen



## **Engineering Education and Research Using MATLAB**

Edited by Dr. Ali Assi

ISBN 978-953-307-656-0

Hard cover, 480 pages

**Publisher** InTech

**Published online** 10, October, 2011

**Published in print edition** October, 2011

MATLAB is a software package used primarily in the field of engineering for signal processing, numerical data analysis, modeling, programming, simulation, and computer graphic visualization. In the last few years, it has become widely accepted as an efficient tool, and, therefore, its use has significantly increased in scientific communities and academic institutions. This book consists of 20 chapters presenting research works using MATLAB tools. Chapters include techniques for programming and developing Graphical User Interfaces (GUIs), dynamic systems, electric machines, signal and image processing, power electronics, mixed signal circuits, genetic programming, digital watermarking, control systems, time-series regression modeling, and artificial neural networks.

### **How to reference**

In order to correctly reference this scholarly work, feel free to copy and paste the following:

John M. Hutchinson and Iria Fraga (2011). The Use of Matlab in the Study of the Glass Transition and Vitrification in Polymers, Engineering Education and Research Using MATLAB, Dr. Ali Assi (Ed.), ISBN: 978-953-307-656-0, InTech, Available from: <http://www.intechopen.com/books/engineering-education-and-research-using-matlab/the-use-of-matlab-in-the-study-of-the-glass-transition-and-vitrification-in-polymers>

**INTECH**  
open science | open minds

### **InTech Europe**

University Campus STeP Ri  
Slavka Krautzeka 83/A  
51000 Rijeka, Croatia  
Phone: +385 (51) 770 447  
Fax: +385 (51) 686 166  
[www.intechopen.com](http://www.intechopen.com)

### **InTech China**

Unit 405, Office Block, Hotel Equatorial Shanghai  
No.65, Yan An Road (West), Shanghai, 200040, China  
中国上海市延安西路65号上海国际贵都大饭店办公楼405单元  
Phone: +86-21-62489820  
Fax: +86-21-62489821

© 2011 The Author(s). Licensee IntechOpen. This is an open access article distributed under the terms of the [Creative Commons Attribution 3.0 License](#), which permits unrestricted use, distribution, and reproduction in any medium, provided the original work is properly cited.

IntechOpen

IntechOpen